Hindawi Publishing Corporation
Abstract and Applied Analysis
Volume 2013, Article ID 152459, 19 pages
http://dx.doi.org/10.1155/2013/152459

Research Article

Stability and Bifurcation Analysis of a Delayed Leslie-Gower Predator-Prey System with Nonmonotonic Functional Response

Jiao Jiang[1] and Yongli Song[2]

[1] *Department of Mathematics, Shanghai Maritime University, Shanghai 201306, China*
[2] *Department of Mathematics, Tongji University, Shanghai 200092, China*

Correspondence should be addressed to Yongli Song; 05143@tongji.edu.cn

Received 21 December 2012; Accepted 7 April 2013

Academic Editor: Kunquan Lan

A delayed Leslie-Gower predator-prey model with nonmonotonic functional response is studied. The existence and local stability of the positive equilibrium of the system with or without delay are completely determined in the parameter plane. Using the method of upper and lower solutions and monotone iterative scheme, a sufficient condition independent of delay for the global stability of the positive equilibrium is obtained. Hopf bifurcations induced by the ratio of the intrinsic growth rates of the predator and prey and by delay, respectively, are found. Employing the normal form theory, the direction and stability of Hopf bifurcations can be explicitly determined by the parameters of the system. Some numerical simulations are given to support and extend our theoretical results. Two limit cycles enclosing an equilibrium, one limit cycle enclosing three equilibria and different types of heteroclinic orbits such as connecting two equilibria and connecting a limit cycle and an equilibrium are also found by using analytic and numerical methods.

1. Introduction

Predation is one of the most fundamental interactions between different species and is universal in nature. Recent studies have shown that predator-prey relationships (not competitive or mutualistic relationships) provide the necessary stability for almost infinite numbers of species to exist in ecosystems and make the rich biodiversity of complex ecosystems possible [1]. The mathematical model and the related dynamics are very useful for qualitatively understanding the interaction between predators and preys. Thus, the predator-prey dynamics has been extensively studied and continue to be of interest to both applied mathematicians and ecologists.

The pioneering predator-prey model was initially proposed by Lotka [2] and Volterra [3] (known as Lotka-Volterra predator-prey model) and successfully captured the oscillations in populations of a predator and its prey. Holling extended this model in [4–6] where various types of functional responses were proposed to better understand the components of predator-prey interactions. The Lotka-Volterra predator-prey model with Holling functional response has been a cornerstone in the field of mathematical biology, and much literature has been devoted to study variants of these equations.

Another important type of well-known predator-prey models was initially proposed and studied by Leslie and Gower [7–9]. Compared with Lotka-Volterra model, the novel feature of Leslie-Gower model is that both interacting species are assumed to grow according to the logistic law, the environmental carrying capacity of the predator is not a constant but a function of the available prey quantity, that there are upper limits to the rates of increase of both prey and predator, which are not recognized in the Lotka-Volterra model. Later, Holling functional response was introduced to Leslie-Gower model by May [10] and the corresponding model is described by the following ordinary differential equations:

$$\begin{aligned} \dot{x} &= rx\left(1-\frac{x}{K}\right)-p(x)\,y, \\ \dot{y} &= s\left(1-\frac{y}{nx}\right)y, \end{aligned} \tag{1}$$

where $x(t)$ and $y(t)$ denote the prey and predator densities, respectively, $p(x)$ represents the Holling type functional

response [6], the positive constants r and s are the intrinsic growth rates of the prey and predators, respectively, the carrying capacity for the prey is a positive constant K, n is a measure of the food quality that the prey provides for conversion into predator births, and then nx is considered as the carrying capacity for the predator. The model (1) is also known as the Holling-Tanner predator-prey model [11–13]. When the functional response $p(x)$ is Holling types I, II, and III functions respectively, it has been proven that the dynamics of model (1) are quite interesting and the global stability of the positive equilibrium, the existence of limit cycles, and so forth have been investigated by many researchers (see, e.g., [12–16] and references therein). Holling type I, II, and III functional responses are similar in that each per capita rate of predation increases with prey density to a maximum [4] and it is shown that the model (1) with the type I, II, and III functional responses exhibits qualitatively similar bifurcation and stability behavior [17]. Holling type IV functional response described by Holling in [18] incorporates prey interference with predation. The main characteristic of Holling type IV functional response is that the per capita predation rate increases with prey density to a maximum at a critical prey density beyond which it decreases, while for other Holling functional responses, the per capita predation rate always increases with prey density. Collings [17] has also numerically shown that the dynamics of the model (1) with Holling type IV functional response is very different from that of the model (1) with other Holling functional responses at higher levels of prey interference. The qualitative analysis for the model (1) with a simplified Holling type IV functional response, proposed by Sokol and Howell [19] as follows:

$$p(x) = \frac{mx}{a + x^2}, \tag{2}$$

has been studied by Li and Xiao [20]. They mainly studied the case when the model has two equilibria: one is an unstable multiple focus with multiplicity one and the other is a cusp of codimension 2 and the dynamics of the model near the small neighborhoods of these two equilibria.

On the other hand, the introduction of time delay into the population model is more realistic to model the interaction between the predator and prey populations and the population models with time delay are of current research interest in mathematical biology [21, 22]. There is extensive literature about the effects of delay on the dynamics of predator-prey models. We refer to a recent survey paper by Ruan [22] and the references cited therein for studies on delayed Lotka-Volterra predator-prey models with Holling functional response. The effects of delay on the dynamics of the Leslie-Gower predator-prey model with and its modified version have been recently studied by many authors (see, e.g., [23–26] and references therein). However, most of them considered the case of the monotonic functional response, under which the corresponding system has only one positive equilibrium. When the nonmonotonic functional response (Holling type IV) is introduced to the Leslie-Gower predator-prey model, there is a possibility of the existence of one, two or three positive equilibria and the dynamics is much more complex [17, 20]. In [27], the authors considered the following delayed Leslie-Gower model with nonmonotonic functional response:

$$\begin{aligned} x'(t) &= rx(t)\left(1 - \frac{x(t)}{k_1}\right) - \frac{mx(t)}{a + x^2(t)}y(t), \\ y'(t) &= y(t)\left[s\left(1 - h\frac{y(t-\tau)}{x(t-\tau) + k_2}\right)\right], \end{aligned} \tag{3}$$

where τ is incorporated because of the negative feedback of the predator density. Under the assumption that the positive equilibrium exists and it is stable for $\tau = 0$, the local stability and delay-induced Hopf bifurcations have been investigated. The supercritical stable Hopf bifurcations were also found by normal form theory and numerical simulation.

In this paper, following the work of Li and Xiao [20] and Lian and Xu [27], we study how the hunting delay affects the dynamics of the Leslie-Gower predator-prey model nonmonotonic functional response. Introducing the hunting delay into the Leslie-Gower predator-prey model with nonmonotonic functional response, we have the following delay differential equations:

$$\begin{aligned} x'(t) &= rx(t)\left(1 - \frac{x(t)}{K}\right) - \frac{mx(t)\,y(t-\tau)}{x^2(t) + a}, \\ y'(t) &= s\left(1 - \frac{y(t)}{nx(t)}\right)y(t), \end{aligned} \tag{4}$$

where the biologic meaning of the parameters r, s, n is the same as in model (1), m is the maximal predator per capita consumption rate, that is, the maximum number of prey that can be eaten by a predator in each time unit, and a is the number of prey necessary to achieve one-half of the maximum rate m. To the best of our knowledge, although the dynamics of the delayed Lotka-Volterra predator-prey model with nonmonotonic functional response has been studied in [28, 29], there are a few research papers on the dynamics of the delayed Leslie-Gower predator-prey model (4). Our goal is to obtain the explicit condition for the existence of the positive equilibrium, to investigate the local and global stability, and to study how the hunting delay affects the stability of the positive equilibrium and induces the Hopf bifurcations and their properties.

The paper is organized as follows. In Section 2, we study the explicit condition for the existence of the positive equilibria and their stability and the Hopf bifurcation induced by the intrinsic growth rate of the predator for the system without delay. In Section 3, we investigate the effect of the delay on the dynamics of the system. The local stability is studied by analyzing the related characteristic equation and the global stability is studied by the method of upper and lower solutions and monotone iterative scheme, and the direction and stability of the delay-induced Hopf bifurcation are determined by using the normal form theory. Numerical simulations are performed to illustrate and extend the obtained results in Section 4. A brief discussion is given in Section 5 to conclude the paper.

2. Linear Stability and Hopf Bifurcation Analysis for the System without Delay

In order to reduce the number of parameters and simplify the calculus in system (4), introducing new variables

$$\bar{t} = rt, \qquad \bar{x}(\bar{t}) = \frac{x(t)}{K}, \qquad \bar{y}(\bar{t}) = \frac{my(t)}{rK^2}, \qquad \bar{\tau} = r\tau \tag{5}$$

and then dropping the bars, we derive

$$\begin{aligned} \dot{x}(t) &= x(t)(1 - x(t)) - \frac{x(t)\,y(t-\tau)}{x^2(t) + \alpha}, \\ \dot{y}(t) &= \gamma\left(1 - \frac{y(t)}{\beta x(t)}\right) y(t), \end{aligned} \tag{6}$$

where $\alpha = a/K^2$, $\beta = mn/Kr$, and $\gamma = s/r$ are positive parameters. When $\tau = 0$, system (6) becomes the following ordinary differential equations:

$$\begin{aligned} \dot{x}(t) &= x(t)(1 - x(t)) - \frac{x(t)\,y(t)}{x^2(t) + \alpha}, \\ \dot{y}(t) &= \gamma\left(1 - \frac{y(t)}{\beta x(t)}\right) y(t). \end{aligned} \tag{7}$$

Systems (6) and (7) have the same equilibria, but the stability of system (6) is affected by delay. We first consider the existence of equilibria and their stability for system (7).

2.1. Existence of Equilibria and Their Stability. From the biological viewpoint, we are only interested in the dynamics of system (7) in the closed first quadrant R_+^2 in the (x, y) plane. Letting $E^*(x^*, y^*)$ denote the equilibrium of system (7), then (x^*, y^*) are the positive real roots of the following equations:

$$1 - x = \frac{y}{x^2 + \alpha}, \quad y = \beta x. \tag{8}$$

We first have the following results on the existence of the positive equilibrium of system (7).

Lemma 1. *(i) If $\alpha \geq 1/27$, then system (7) has a unique positive equilibrium.*

(ii) If $0 < \alpha < 1/27$, then system (7) has three positive equilibria for $\beta_1(\alpha) < \beta < \beta_2(\alpha)$, two positive equilibria for $\beta = \beta_1(\alpha)$ or $\beta = \beta_2(\alpha)$, and a unique positive equilibrium for $\beta < \beta_1(\alpha)$ or $\beta > \beta_2(\alpha)$, where $\beta_j(\alpha) = -3T_j^2 + 2T_j - \alpha$, $j = 1, 2$, with

$$\begin{aligned} T_1 &= \frac{1 + \cos(\arccos(-1 + 54\alpha)/3)}{6} \\ &\quad - \frac{\sqrt{3}\sin(\arccos(-1 + 54\alpha)/3)}{6}, \\ T_2 &= \frac{1 + \cos(\arccos(-1 + 54\alpha)/3)}{6} \\ &\quad + \frac{\sqrt{3}\sin(\arccos(-1 + 54\alpha)/3)}{6}. \end{aligned} \tag{9}$$

Proof. (i) From (8), we have $(1 - x)(x^2 + \alpha) = \beta x$. Let $y_1(x) = (1-x)(x^2+\alpha)$, and $y_2(x) = \beta x$. Notice that $y_1(0) = \alpha > 0$ and $y_1(x)$ is decreasing as the x-value increases for $\alpha \geq 1/3$ since $y_1'(x) = -3x^2 + 2x - \alpha \leq 0$ for $\alpha \geq 1/3$. So, when $\alpha \geq 1/3$, the two curves $y_1(x)$ and $y_2(x)$ have only one interaction point for $x > 0$ and $\beta > 0$.

When $0 < \alpha < 1/3$, the curve $y_1(x)$ has one minimum at $x = m_*$ and one maximum at $x = m^*$ and decreases in the interval $x \in (0, m_*) \cup (m^*, 1)$ and increases in the interval (m_*, m^*), where

$$m_* = \frac{1 - \sqrt{1 - 3\alpha}}{3}, \qquad m^* = \frac{1 + \sqrt{1 - 3\alpha}}{3}. \tag{10}$$

The tangent point of two curves $y_1(x)$ and $y_2(x)$ is the key point for determining how many intersection points of these two curves. The tangent point of two curves $y_1(x)$ and $y_2(x)$ can be determined by the roots of the following equations

$$\begin{aligned} (1 - x)\left(\alpha + x^2\right) &= \beta x, \\ -3x^2 + 2x - \alpha &= \beta, \end{aligned} \tag{11}$$

which yields

$$2x^3 - x^2 + \alpha = 0. \tag{12}$$

It is easy to verify that the function $p(x) = 2x^3 - x^2 + \alpha$ has a minimum at $x = 1/3$ for $x > 0$. Noticing that $p(1/3) = 0$ is equivalent to $\alpha = 1/27$, we can deduce that (12) has no positive real roots for $1/27 < \alpha < 1/3$, one positive real root for $\alpha = 1/27$, and two different positive real roots for $0 < \alpha < 1/27$. Thus, when $1/27 < \alpha < 1/3$, the straight line $y_2(x)$ is not tangent to the curve $y_1(x)$ for any $x > 0$ and $\beta > 0$. When $\alpha = 1/27$, the straight line $y_2(x)$ is tangent to the curve $y_1(x)$ only at $\beta = 8/27$ and $x = 1/3$, as shown in Figure 1(a). Consequently, when $1/27 \leq \alpha < 1/3$, the two curves $y_1(x)$ and $y_2(x)$ have only one interaction point for any $x > 0$ and $\beta > 0$. This completes the proof of conclusion (i).

(ii) When $0 < \alpha < 1/27$, it follows from Shengjin's theorem [30] that the two positive real roots of (12) are T_1 and T_2 defined by (9). This, together with (11), implies that two curves $y_1(x)$ and $y_2(x)$ are tangent at points $\beta_j = -3T_j^2 + 2T_j - \alpha$, $j = 1, 2$, as shown in Figure 1(b) for $\alpha = 1/40$. This completes the proof of conclusion (ii). □

According to Lemma 1, the distribution of the positive equilibria of system (7) in the α-β plane can be illustrated in Figure 2.

The Jacobian matrix of system (7) at the positive equilibrium point E^* is

$$J = \begin{pmatrix} -r_1 & -r_2 \\ \beta\gamma & -\gamma \end{pmatrix}, \tag{13}$$

where

$$r_1 = -\frac{x^* y_1'(x^*)}{(x^*)^2 + \alpha}, \qquad r_2 = \frac{x^*}{(x^*)^2 + \alpha} > 0. \tag{14}$$

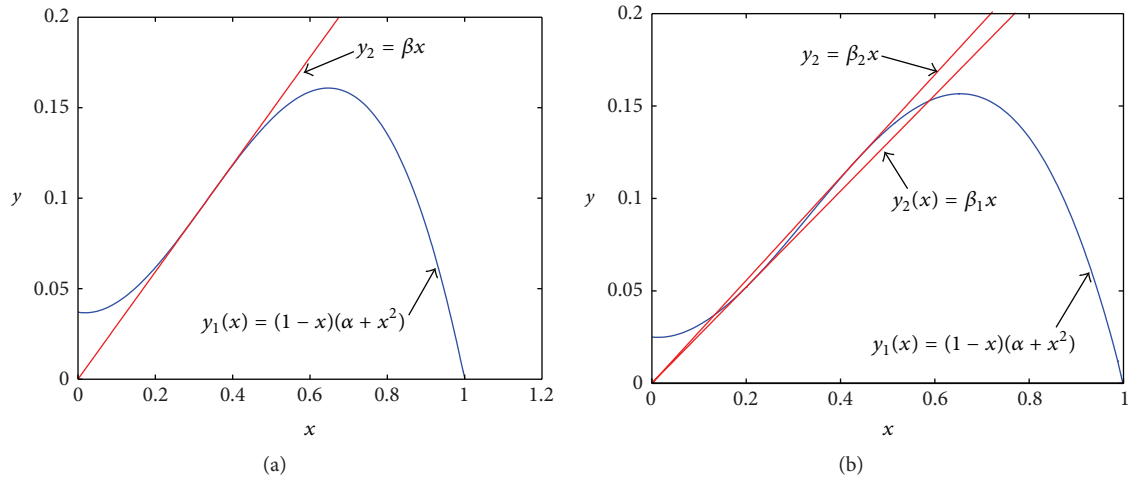

Figure 1: Diagram of positive equilibrium. (a) When $\alpha \geq 1/27$, there exists only one positive equilibrium for any $\beta > 0$. Here, $\alpha = 1/27$, and $\beta = 8/27$. (b) When $0 < \alpha < 1/27$, there are three cases: (i) only one positive equilibrium for $\beta < \beta_1$ or $\beta > \beta_2$, (ii) two positive equilibria for $\beta = \beta_1$ or $\beta = \beta_2$, and (iii) three positive equilibria for $\beta_1 < \beta < \beta_2$. Here, $\alpha = 1/40$, $\beta_1 = 0.2599$, and $\beta_2 = 0.2782$.

Then the characteristic equation at E^* is

$$\lambda^2 + (r_1 + \gamma)\lambda + \gamma(r_1 + r_2\beta) = 0. \tag{15}$$

Letting β_1^* and β_2^* denote the slopes of the straight line $y_2(x)$ crossing the maximum and minimum points of $y_1(x)$, respectively, we have

$$\beta_1^* = \frac{(1 - m^*)\left(\alpha + (m^*)^2\right)}{m^*}, \qquad \beta_2^* = \frac{(1 - m_*)\left(\alpha + m_*^2\right)}{m_*}, \tag{16}$$

where m_* and m^* are defined by (10). When $\alpha < 1/3$, we have $\beta_1^* < \beta_2^*$, as shown in Figure 2. The curves β_1, β_2, β_1^*, β_2^* divide the α-β plane into four regions D_i, $i = 1, 2, 3, 4$, as shown in Figure 2. From Lemma 1, we know that system (7) has only one positive equilibrium in the regions D_1 and D_2, two positive equilibria in the curves $\beta_1(\alpha)$ and $\beta_2(\alpha)$ with $\alpha \leq 1/27$, three positive equilibria in the regions D_3 and D_4. Notice that

$$r_1 = -\frac{x^* y_1'(x^*)}{(x^*)^2 + \alpha}, \qquad r_1 + r_2\beta = \frac{x^*}{(x^*)^2 + \alpha}\left(\beta - y_1'(x^*)\right), \tag{17}$$

and then by a direct but tedious analysis, we have the following results on the signs of r_1 and $r_1 + r_2\beta$, which determine the stability of the positive equilibrium.

In the regions D_1 and D_2, we have

$$r_1 \begin{cases} > 0, & \text{for } (\alpha, \beta) \in D_1, \\ = 0, & \text{for } (\alpha, \beta) \text{ lying on the curves } \beta_1^*(\alpha) \text{ or } \beta_2^*(\alpha), \\ < 0, & \text{for } (\alpha, \beta) \in D_2, \end{cases} \qquad r_1 + r_2\beta > 0. \tag{18}$$

In the regions D_3 and D_4, denote the three positive equilibria by $E_i^*(x_i^*, y_i^*)$, $i = 1, 2, 3$ with $x_1^* < x_2^* < x_3^*$. Notice that $x_1^* < T_1$, $T_1 < x_2^* < T_2$, $x_3^* > T_2$. Then we have

$$r_1 \begin{cases} < 0, & \text{for } (\alpha, \beta) \in D_3, \text{ all three equilibria } E_i^*,\ i = 1, 2, 3, \\ < 0, & \text{for } (\alpha, \beta) \in D_4, \text{ the equilibria } E_1^* \text{ and } E_2^*, \\ > 0, & \text{for } (\alpha, \beta) \in D_4, \text{ the equilibria } E_3^*, \end{cases} \tag{19}$$

$$r_1 + r_2\beta \begin{cases} < 0, & \text{for } E_2^*, \\ > 0, & \text{for } E_1^* \text{ and } E_3^*. \end{cases} \tag{20}$$

In addition, notice that if $r_1 \geq 0$, then $r_1 + \gamma > 0$ for any $\gamma > 0$. However, when $r_1 < 0$, we can choose γ as a parameter such that $r_1 + \gamma \geq 0$ for $\gamma \geq -r_1$ and $r_1 + \gamma < 0$ for $0 < \gamma < -r_1$. Thus, by (18), (19), and (20), we have the following results on the distribution of roots of (15).

Lemma 2. *Assume that T_1, T_2 are defined by* (9) *and $\gamma_0 = x^* y_1'(x^*)/((x^*)^2 + \alpha)$.*

(i) *In the region D_1, for the unique equilibrium E^*, all roots of* (15) *have negative real parts for any $\gamma > 0$.*

(ii) *In the region D_2, for the unique equilibrium E^*, all roots of* (15) *have negative real parts for $\gamma > \gamma_0$, a pair of purely imaginary roots $\pm i\sqrt{\gamma_0(r_1 + r_2\beta)}$ at $\gamma = \gamma_0$, and* (15) *has at least a root with positive real part for $0 < \gamma < \gamma_0$.*

(iii) *In the region D_3, for the positive equilibrium E_2^*,* (15) *has at least a root with positive real part for any $\gamma > 0$; for other two positive equilibria E_1^* and E_3^*, all roots of* (15) *have negative real parts for $\gamma > \gamma_0$, a pair of purely imaginary roots $\pm i\sqrt{\gamma_0(r_1 + r_2\beta)}$ at $\gamma = \gamma_0$, and* (15) *has at least a root with positive real part for $0 < \gamma < \gamma_0$.*

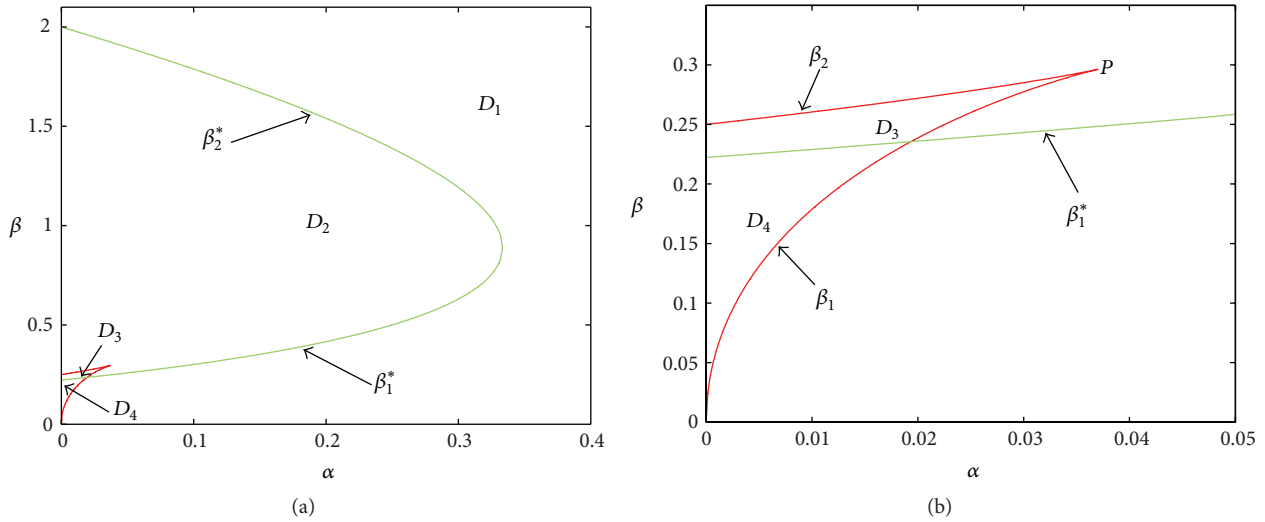

FIGURE 2: Bifurcation diagram of positive equilibrium in the α-β plane. System (7) has three positive equilibria in the inner region enclosed by the curves β_1 and β_2, a unique positive equilibrium outside this region and on the point $P(1/27, 8/27)$ and two positive equilibria on the two curves on the boundary curves β_1 and β_2 except the point $P(1/27, 8/27)$.

(iv) *In the region D_4, for the positive equilibrium E_2^*, (15) has at least a root with positive real part for any $\gamma > 0$; for the positive equilibrium E_1^*, all roots of (15) have negative real parts for $\gamma > \gamma_0$, a pair of purely imaginary roots $\pm i\sqrt{\gamma_0(r_1 + r_2\beta)}$ at $\gamma = \gamma_0$, and (15) has at least a root with positive real part for $0 < \gamma < \gamma_0$; for the positive equilibrium E_3^*, all roots of (15) have negative real parts for any $\gamma > 0$.*

Taking γ as a parameter and letting λ is a root of (15) such that $\mathrm{Re}(\lambda(\gamma_0)) = 0$ and $\mathrm{Im}(\lambda(\gamma_0)) = \sqrt{\gamma_0(r_1 + r_2\beta)}$. A straight calculation yields the following transversality condition:

$$\begin{aligned}\left.\frac{d\,\mathrm{Re}(\lambda)}{d\gamma}\right|_{\gamma=\gamma_0} &= \mathrm{Re}\left\{-\frac{\lambda + r_1 + r_2\beta}{2\lambda + r_1 + \gamma}\right\}\Bigg|_{\gamma=\gamma_0} \\ &= \mathrm{Re}\left\{-\frac{1}{2} - \frac{r_1 + r_2\beta}{2\lambda}\right\}\Bigg|_{\gamma=\gamma_0} = -\frac{1}{2} < 0.\end{aligned} \tag{21}$$

From Lemma 2 and the transversality condition (21), the following theorem on the stability and bifurcation follows immediately.

Theorem 3. *Assuming that T_1, T_2 are defined by (9) and $\gamma_0 = x^* y_1'(x^*)/((x^*)^2 + \alpha)$.*

(i) *In the region D_1, the unique equilibrium E^* is asymptotically stable for any $\gamma > 0$.*

(ii) *In the region D_2, the unique equilibrium E^* is asymptotically stable for $\gamma > \gamma_0$ and unstable for $0 < \gamma < \gamma_0$, and system (7) undergoes Hopf bifurcation at $\gamma = \gamma_0$.*

(iii) *In the region D_3, the positive equilibrium E_2^* is unstable for any $\gamma > 0$; other two positive equilibria E_1^* and E_3^* are asymptotically stable for $\gamma > \gamma_0$ and unstable for $0 < \gamma < \gamma_0$, the and system (7) undergoes Hopf bifurcation near neighborhood of each of these two equilibria at $\gamma = \gamma_0$.*

(iv) *In the region D_4, the positive equilibrium E_2^* is unstable for any $\gamma > 0$; the positive equilibrium E_1^* is asymptotically stable for $\gamma > \gamma_0$ and unstable for $0 < \gamma < \gamma_0$, and system (7) undergoes Hopf bifurcation near neighborhood of E_1^* at $\gamma = \gamma_0$; the positive equilibrium E_3^* is asymptotically stable for any $\gamma > 0$.*

2.2. Direction and Stability of Hopf Bifurcation Associated with γ_0. It follows from Theorem 3 that when $(\alpha, \beta) \in D_i$, $i = 2, 3, 4$, Hopf bifurcation occurs at $\gamma = \gamma_0$. When Hopf bifurcation occurs, the corresponding characteristic equation has a pair of purely imaginary roots at $\gamma = \gamma_0$ and thus the linearization is not sufficient to determine the stability of the corresponding equilibrium, say, E^*. In this subsection, by calculating the focal value we determine the stability of the equilibrium E^* at $\gamma = \gamma_0$, which is directly associated with the direction and stability of Hopf bifurcation associated with γ_0.

Assume that $\lambda_{1,2} = \eta(\gamma) \pm i\varpi(\gamma)$ are a pair of complex conjugates of (15) such that $\eta(\gamma_0) = 0$, $\varpi(\gamma_0) = \sqrt{\gamma_0(r_1 + r_2\beta)}$. Then the eigenvector corresponding to $\lambda_{1,2}$ is

$$\begin{pmatrix} 1 \\ -\dfrac{r_1 + \eta(\gamma) \pm i\varpi(\gamma)}{r_2} \end{pmatrix}. \tag{22}$$

Under the following coordinate transformation:

$$\begin{pmatrix} z_1 \\ z_2 \end{pmatrix} = \begin{pmatrix} 1 & 0 \\ M & N \end{pmatrix} \begin{pmatrix} u \\ v \end{pmatrix}, \tag{23}$$

where $M = -(r_1 + \eta(\gamma))/r_2$, $N = \varpi(\gamma)/r_2$, system (7) becomes

$$\begin{pmatrix} \dot{u}(t) \\ \dot{v}(t) \end{pmatrix} = J(\gamma) \begin{pmatrix} u(t) \\ v(t) \end{pmatrix} + \begin{pmatrix} F^{(1)}(u, v, \gamma) \\ F^{(2)}(u, v, \gamma) \end{pmatrix}, \tag{24}$$

where

$$J(\gamma) = \begin{pmatrix} \eta(\gamma) & -\varpi(\gamma) \\ \varpi(\gamma) & \eta(\gamma) \end{pmatrix} \tag{25}$$

with

$$\begin{aligned} F^{(1)}(u,v,\gamma) = {} & \left(\frac{1}{2}f_{20}^{(1)} + Mf_{11}^{(1)}\right)u^2 + Nf_{11}^{(1)}uv \\ & + \left(\frac{1}{6}f_{30}^{(1)} + \frac{1}{2}Mf_{21}^{(1)}\right)u^3 \\ & + \frac{1}{2}Nf_{21}^{(1)}u^2v + O\left(|u,v|^4\right), \\ F^{(2)}(u,v,\gamma) = {} & -\frac{M}{N}F^{(1)}(u,v,\gamma) + \frac{1}{N}\widehat{F}^{(2)}(u,v,\gamma), \end{aligned} \tag{26}$$

where

$$\begin{aligned} \widehat{F}^{(2)}(u,v,\gamma) = {} & \left(\frac{1}{2}f_{20}^{(2)} + Mf_{11}^{(2)} + \frac{1}{2}M^2f_{02}^{(2)}\right)u^2 \\ & + \left(Nf_{11}^{(2)} + MNf_{02}^{(2)}\right)uv + \frac{1}{2}N^2f_{02}^{(2)}v^2 \\ & + \left(\frac{1}{6}f_{30}^{(2)} + \frac{1}{2}Mf_{21}^{(2)} + \frac{1}{2}M^2f_{12}^{(2)}\right)u^3 \\ & + \left(\frac{1}{2}Nf_{21}^{(2)} + MNf_{12}^{(2)}\right)u^2v \\ & + \frac{1}{2}N^2f_{12}^{(2)}uv^2 + O\left(|u,v|^4\right). \end{aligned} \tag{27}$$

Find $f_{ij}^{(1)}$ and $f_{ij}^{(2)}$ at (31). By the formula for the third focal value of a multiple focus in [31], we have

$$\begin{aligned} a_3(\gamma_0) = {} & \frac{1}{16}\left(F_{uuu}^{(1)} + F_{uvv}^{(1)} + F_{uuv}^{(2)} + F_{vvv}^{(2)}\right)\Big|_{(0,0,\gamma_0)} \\ & + \frac{1}{16\varpi(\gamma_0)}\left(F_{uv}^{(1)}\left(F_{uu}^{(1)} + F_{vv}^{(1)}\right)\right. \\ & - F_{uv}^{(2)}\left(F_{uu}^{(2)} + F_{vv}^{(2)}\right) \\ & \left. -F_{uu}^{(1)}F_{uu}^{(2)} + F_{vv}^{(1)}F_{vv}^{(2)}\right)\Big|_{(0,0,\gamma_0)}, \end{aligned} \tag{28}$$

where

$$\begin{aligned} & F_{uuu}^{(1)} = f_{30}^{(1)} + 3Mf_{21}^{(1)}, \qquad F_{uvv}^{(1)} = 0, \\ & F_{uuv}^{(2)} = -Mf_{21}^{(1)} + f_{21}^{(2)} + 2Mf_{12}^{(2)}, \qquad F_{vvv}^{(2)} = 0, \\ & F_{uv}^{(1)} = Nf_{11}^{(1)}, \qquad F_{uu}^{(1)} = f_{20}^{(1)} + 2Mf_{11}^{(1)}, \\ & F_{vv}^{(1)} = 0, \qquad F_{uv}^{(2)} = -Mf_{11}^{(1)} + f_{11}^{(2)} + Mf_{02}^{(2)}, \\ & F_{vv}^{(2)} = N^2f_{02}^{(2)}, \\ & F_{uu}^{(2)} = -\frac{M}{N}\left(\frac{1}{2}f_{20}^{(1)} + Mf_{11}^{(1)}\right) \\ & \quad + \frac{1}{N}\left(\frac{1}{2}f_{20}^{(2)} + Mf_{11}^{(2)} + \frac{1}{2}M^2f_{02}^{(2)}\right). \end{aligned} \tag{29}$$

It is well known from the result in [31] that if $a_3(\gamma_0) < 0$, then the equilibrium E^* of system (7) is a stable multiple focus of multiplicity 1 and the corresponding Hopf bifurcation is supercritical, and if $a_3(\gamma_0) > 0$, then the equilibrium E^* of system (7) is an unstable multiple focus of multiplicity 1 and the corresponding Hopf bifurcation is subcritical.

3. Stability and Hopf Bifurcation Analysis for the System with Delay

In this section, we focus on the investigation of the local stability and Hopf bifurcation criteria of the positive equilibrium $E^*(x^*, y^*)$ for the system (6). Letting $z_1(t) = x(t) - x^*$ and $z_2(t) = y(t) - y^*$, we can rewrite the system (6) by Taylor series expression about (x^*, y^*) as the following system:

$$\begin{aligned} z_1'(t) = {} & -r_1z_1(t) - r_2z_2(t-\tau) \\ & + \sum_{i+j\geq 2}\frac{1}{i!\,j!}f_{ij}^{(1)}z_1^i(t)\,z_2^j(t-\tau), \\ z_2'(t) = {} & \beta\gamma z_1(t) - \gamma z_2(t) + \sum_{i+j\geq 2}\frac{1}{i!\,j!}f_{ij}^{(2)}z_1^i(t)\,z_2^j(t), \end{aligned} \tag{30}$$

where

$$\begin{aligned} & r_1 = -\frac{x^*y_1'(x^*)}{(x^*)^2 + \alpha}, \qquad r_2 = \frac{x^*}{(x^*)^2 + \alpha} > 0, \\ & f_{ij}^{(1)} = \left.\frac{\partial^{i+j}f^{(1)}}{\partial x^i\partial y^j}\right|_{(x^*,y^*)}, \qquad f_{ij}^{(2)} = \left.\frac{\partial^{i+j}f^{(2)}}{\partial x^i\partial y^j}\right|_{(x^*,y^*)}, \\ & f^{(1)} = x(1-x) - \frac{xy}{x^2+\alpha}, \qquad f^{(2)} = \gamma\left(1 - \frac{y}{\beta x}\right)y. \end{aligned} \tag{31}$$

3.1. Linear Stability and Delay-Induced Hopf Bifurcation. The characteristic equation at E^* takes the form

$$\lambda^2 + (r_1 + \gamma)\lambda + \gamma r_1 + \gamma r_2\beta e^{-\lambda\tau} = 0. \tag{32}$$

When the time delay $\tau = 0$, the equilibrium $E(x^*, y^*)$ is asymptotically stable if

$$r_1 + \gamma > 0, \qquad r_1 + r_2\beta > 0. \tag{33}$$

Now for $\tau > 0$, assuming that $\lambda = i\omega(\omega > 0)$ is a root of (32), then we have

$$-\omega^2 + (r_1 + \gamma)i\omega + \gamma r_1 + \gamma r_2\beta e^{-i\omega\tau} = 0. \tag{34}$$

Separating the real and imaginary parts, we obtain

$$\begin{aligned} \omega^2 - \gamma r_1 &= \gamma r_2\beta\cos(\omega\tau), \\ (r_1 + \gamma)\omega &= \gamma r_2\beta\sin(\omega\tau), \end{aligned} \tag{35}$$

which leads to the following fourth degree polynomial equation:

$$\omega^4 + \left(r_1^2 + \gamma^2\right)\omega^2 + \gamma^2r_1^2 - \gamma^2r_2^2\beta^2 = 0. \tag{36}$$

It is easy to see that if

$$r_1^2 - r_2^2\beta^2 < 0, \tag{37}$$

then (36) has only one positive root

$$\omega_0 = \sqrt{\frac{-\left(r_1^2+\gamma^2\right) + \sqrt{\left(r_1^2-\gamma^2\right)^2 + 4\gamma^2 r_2^2\beta^2}}{2}}. \tag{38}$$

Substituting the value of ω_0 in (35) and solve for τ, we get

$$\tau_j = \frac{1}{\omega_0}\arccos\left(\frac{\omega_0^2 - \gamma r_1}{\gamma r_2\beta}\right) + \frac{2j\pi}{\omega_0}, \quad j = 0, 1, \ldots \tag{39}$$

then when $\tau = \tau_j$, the characteristic equation (32) has a pair of purely imaginary roots $\pm i\omega_0$.

Let $\lambda(\tau) = \zeta(\tau) + i\omega(\tau)$ be a root of (32) such that the following two conditions hold:

$$\zeta\left(\tau_j\right) = 0, \qquad \omega\left(\tau_j\right) = \omega_0. \tag{40}$$

Substituting $\lambda(\tau) = \zeta(\tau)+i\omega(\tau)$ into (32) and taking the derivative of resulting expression with respect to τ, we get

$$\frac{d\lambda}{d\tau} = \frac{\lambda\gamma r_2\beta e^{-\lambda\tau}}{2\lambda + r_1 + \gamma - \tau\gamma r_2\beta e^{-\lambda\tau}} \tag{41}$$

which, together with (35) and (38), leads to

$$\begin{aligned}
&\operatorname{sign}\left\{\operatorname{Re}\left[\frac{d\lambda}{d\tau}\right]^{-1}\right\}_{\lambda=i\omega_0} \\
&\quad= \operatorname{sign}\left\{\operatorname{Re}\left[\frac{\left(2\lambda + r_1 + \gamma\right)e^{\lambda\tau}}{\lambda\gamma r_2\beta}\right]\right\}_{\lambda=i\omega_0} \\
&\quad= \operatorname{sign}\left\{\frac{2\omega_0^2 + r_1^2 + \gamma^2}{\gamma^2 r_2^2\beta^2}\right\} > 0.
\end{aligned} \tag{42}$$

Therefore, the transversality condition holds, and hence Hopf-bifurcation occurs at $\tau = \tau_j$. Because the quartic equation (36) has only one positive root, system (6) has no switching stability. Delay-induced small-amplitude period solution bifurcates from interior equilibrium point when τ passes through its critical magnitude $\tau = \tau_0$. Here, τ_0 is the smallest positive value of τ_j given in (39).

To study the effect of the delay on the stability of the interior equilibrium in regions D_i, $i = 1, 2, 3, 4$, we just need decide the sign of $r_1 - r_2\beta$ by (18), (20), and (37). Notice that $r_1 - r_2\beta = -(x^*/((x^*)^2+\alpha))(\beta + y_1'(x^*))$. So we first determine at which point the slope of curve y_1 is negative of the slope of line y_2; that is, we need to find the solution of the following equations:

$$\begin{aligned}
(1-x)\left(\alpha + x^2\right) &= \beta x, \\
-3x^2 + 2x - \alpha + \beta &= 0,
\end{aligned} \tag{43}$$

which yields

$$4x^3 - 3x^2 + 2\alpha x - \alpha = 0. \tag{44}$$

Let $q(x) = 4x^3 - 3x^2 + 2\alpha x - \alpha$. When $\alpha \geq 3/8$, $q'(x) = 12(x - 1/4)^2 - 3/4 + 2\alpha \geq 0$, which implies that the function $q(x)$ is increasing for any $x > 0$. Notice that $q(0) = -\alpha < 0$ and $q(1) = 1 + \alpha > 0$, and we can deduce that (44) has only one positive real root for $\alpha \geq 3/8$. When $0 < \alpha < 3/8$, $q'(x) = 12(x - (3 + \sqrt{9 - 24\alpha})/12)(x - (3 - \sqrt{9 - 24\alpha})/12)$ which implies that the function $q(x)$ has a maximum value at $x_1 = (3 - \sqrt{9 - 24\alpha})/12$ and a minimal value at $x_2 = (3 + \sqrt{9 - 24\alpha})/12$. Furthermore, we can deduce that $q(x_1) = -1/8 + \sqrt{9 - 24\alpha}/24 - \alpha/2 - \alpha\sqrt{9 - 24\alpha}/9 < 0$ and $q(x_2) = -1/8 - \sqrt{9 - 24\alpha}/24 - \alpha/2 + \alpha\sqrt{9 - 24\alpha}/9 < 0$. So (44) has also only one positive real root for $0 < \alpha < 3/8$. By direct computation, the positive real root of (44) is

$$\begin{aligned}
T_3 = \frac{1}{4} &+ \frac{1}{12}\left(27 + 108\alpha + 12\sqrt{96\alpha^3 - 27\alpha^2 + 81\alpha}\right)^{1/3} \\
&- \frac{2\alpha - 3/4}{\left(27 + 108\alpha + 12\sqrt{96\alpha^3 - 27\alpha^2 + 81\alpha}\right)^{1/3}}
\end{aligned} \tag{45}$$

for any $\alpha > 0$. Then $\beta_3 = 3T_3^2 - 2T_3 + \alpha$ divides the regions D_1 and D_4 into two parts, respectively; see Figure 3. When $\beta > \beta_3$, $\beta + y_1'(x^*) > 0$, and when $\beta < \beta_3$, $\beta + y_1'(x^*) < 0$. Therefore,

$$r_1 - r_2\beta \begin{cases} < 0, & \beta > \beta_3, \\ = 0, & \beta = \beta_3, \\ > 0, & \beta < \beta_3. \end{cases} \tag{46}$$

The above results are summarized in the following theorems.

Theorem 4. *(i) In the region D_{11}, for any $\gamma > 0$, the unique equilibrium E^* is asymptotically stable for $\tau \in [0, \tau_0)$ and unstable for $\tau > \tau_0$, and system (6) undergoes Hopf bifurcation near E^* for $\tau = \tau_j$, $j = 0, 1, \ldots$.*

(ii) In the region D_{12}, for any $\gamma > 0$, the unique equilibrium E^* is asymptotically stable for any $\tau \geq 0$.

Theorem 5. *In the region D_2,*

(i) *when $\gamma > \gamma_0$, the unique equilibrium E^* is asymptotically stable for $\tau \in [0, \tau_0)$ and unstable for $\tau > \tau_0$, and system (6) undergoes Hopf bifurcation near E^* for $\tau = \tau_j$, $j = 0, 1, \ldots$;*

(ii) *when $0 < \gamma < \gamma_0$, the unique equilibrium E^* is unstable for any $\tau \geq 0$, and system (6) undergoes Hopf bifurcation near E^* for $\tau = \tau_j$, $j = 0, 1, \ldots$.*

Theorem 6. *In the region D_3,*

(i) *for any $\gamma > 0$, the positive equilibrium E_2^* is unstable for any $\tau \geq 0$;*

(ii) *for other two positive equilibria E_1^* and E_3^*, (a) when $\gamma > \gamma_0$, they are asymptotically stable for $\tau \in [0, \tau_0)$ and unstable for $\tau > \tau_0$, and system (6) undergoes Hopf bifurcation near each of these two equilibria for $\tau = \tau_j$, $j = 0, 1, \ldots$; (b) when $0 < \gamma < \gamma_0$, they are unstable for*

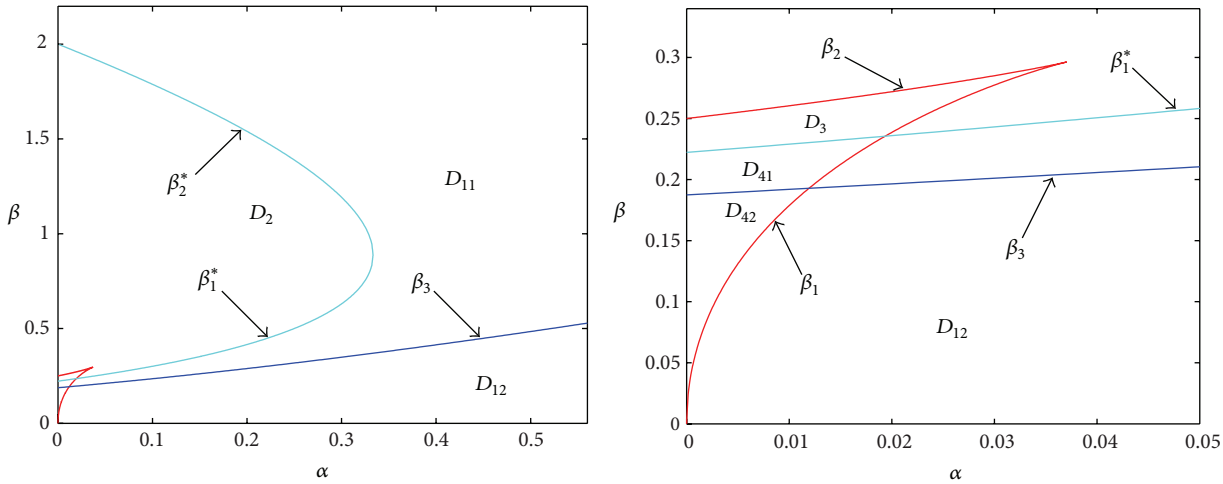

FIGURE 3: Bifurcation diagram of positive equilibrium in the α-β plane. $\beta = \beta_3$ divides D_1 and D_4 into D_{11}, D_{12} and D_{41}, D_{42}, respectively.

any $\tau \geq 0$, and system (6) undergoes Hopf bifurcation near each of these two equilibria for $\tau = \tau_j$, $j = 0, 1, \ldots$.

Theorem 7. *(i) In the region D_{41}, for any $\gamma > 0$, the positive equilibrium E_2^* is unstable for any $\tau \geq 0$; for any $\gamma > 0$, the positive equilibrium E_3^* is asymptotically stable for $\tau \in [0, \tau_0)$ and unstable for $\tau > \tau_0$, and system (6) undergoes Hopf bifurcation near E_3^* for $\tau = \tau_j$, $j = 0, 1, \ldots$; for the positive equilibrium E_1^*, (a) when $\gamma > \gamma_0$, E_1^* is asymptotically stable for $\tau \in [0, \tau_0)$ and unstable for $\tau > \tau_0$, and system (6) undergoes Hopf bifurcation near E_1^* for $\tau = \tau_j$, $j = 0, 1, \ldots$; (b) when $0 < \gamma < \gamma_0$, E_1^* is unstable for any $\tau \geq 0$, and system (6) undergoes Hopf bifurcation near E_1^* for $\tau = \tau_j$, $j = 0, 1, \ldots$.*

(ii) In the region D_{42}, for any $\gamma > 0$, the positive equilibrium E_2^* is unstable for any $\tau \geq 0$, and system (6) undergoes Hopf bifurcation near E_2^* for $\tau = \tau_j$, $j = 0, 1, \ldots$; the positive equilibrium E_1^* is asymptotically stable for $\gamma > \gamma_0$ and unstable for $0 < \gamma < \gamma_0$ for any $\tau \geq 0$; the positive equilibrium E_3^* is asymptotically stable for any $\gamma > 0$ and for any $\tau \geq 0$.

3.2. Global Stability of the Positive Equilibrium. In this section, we give a result on the global stability of the positive equilibrium of system (6).

Theorem 8. *If $\beta < \alpha$, then the unique positive equilibrium $E^*(x^*, y^*)$ of system (6) is global stability. That is, for any initial values $x(t) = \varphi_1(t) \geq 0$, $y(t) = \varphi_2(t) \geq 0$, $t \in [-\tau, 0]$, with $x(0), y(0) > 0$, the corresponding solution $(x(t), y(t))$ of system (6) satisfies*

$$\lim_{t \to \infty} x(t) = x^*, \qquad \lim_{t \to \infty} y(t) = y^*. \tag{47}$$

Proof. By the first equation of system (6), we have $\dot{x}(t) \leq x(t)(1 - x(t))$, which, together with the comparison principle, implies that $\limsup_{t \to +\infty} x(t) \leq 1$. Thus, for any sufficiently small positive number ε_0, there exists $t_1 > 0$ such that for any $t > t_1$,

$$x(t) \leq 1 + \varepsilon_0 \triangleq \overline{c}_1. \tag{48}$$

This, together with the second equation of system (6) yields that for $t > t_1$,

$$\dot{y}(t) \leq \gamma \left(1 - \frac{y(t)}{\beta(1 + \varepsilon_0)}\right) y(t). \tag{49}$$

Again by the comparison principle, we have

$$\liminf_{t \to +\infty} y(t) \leq \beta(1 + \varepsilon_0), \tag{50}$$

which implies that for $\varepsilon_0 > 0$ mentioned above, there exists $t_2 > t_1 > 0$ such that for any $t > t_2$,

$$y(t) \leq \beta(1 + \varepsilon_0) + \varepsilon_0 \triangleq \overline{c}_2. \tag{51}$$

It follows from (51) and the second equation of system (6) that for $t > t_2 + \tau$,

$$\dot{x}(t) \geq x(t)(1 - x(t)) - \frac{\beta(1 + \varepsilon_0) + \varepsilon_0}{\alpha} x(t), \tag{52}$$

which leads to

$$\liminf_{t \to +\infty} x(t) \geq \frac{\alpha - (\beta(1 + \varepsilon_0) + \varepsilon_0)}{\alpha}. \tag{53}$$

So, there exists $t_3 > t_2 > 0$ such that for any $t > t_3$,

$$x(t) \geq \frac{\alpha - (\beta(1 + \varepsilon_0) + \varepsilon_0)}{\alpha} - \varepsilon_0 \triangleq \underline{c}_1. \tag{54}$$

Using this lower bound of x, we obtain

$$\dot{y}(t) \geq \gamma \left(1 - \frac{\alpha}{\beta(\alpha(1 - \varepsilon_0) - (\beta(1 + \varepsilon_0) + \varepsilon_0))} y(t)\right) y(t), \tag{55}$$

which, together with the comparison principle, yields

$$\liminf_{t\to+\infty} y(t) \geq \frac{\beta(\alpha(1-\varepsilon_0)-(\beta(1+\epsilon_0)+\varepsilon_0))}{\alpha}. \tag{56}$$

Therefore, there exists $t_4 > t_3 > 0$ such that for any $t > t_4$,

$$y(t) \geq \frac{\beta(\alpha(1-\varepsilon_0)-(\beta(1+\epsilon_0)+\varepsilon_0))}{\alpha} - \varepsilon_0 \triangleq \underline{c}_2. \tag{57}$$

Clearly, $\overline{c}_1, \overline{c}_2 > 0$. It follows from (54) and (57) that when $\alpha > \beta$, we can choose

$$0 < \varepsilon_0 < \frac{\beta(\alpha-\beta)}{\alpha+\beta(\alpha+\beta+1)} \tag{58}$$

such that $\underline{c}_1, \underline{c}_2 > 0$. By (48)–(57), it is easy to verify that

$$\begin{aligned} 0 &\geq \overline{c}_1(1-\overline{c}_1) - \frac{\overline{c}_1\underline{c}_2}{\overline{c}_1^2+\alpha}, \qquad 0 \geq \gamma\left(1-\frac{\overline{c}_2}{\beta\overline{c}_1}\right)\overline{c}_2, \\ 0 &\leq \underline{c}_1(1-\underline{c}_1) - \frac{\underline{c}_1\overline{c}_2}{\underline{c}_1^2+\alpha}, \qquad 0 \leq \gamma\left(1-\frac{\underline{c}_2}{\beta\underline{c}_1}\right)\underline{c}_2, \end{aligned} \tag{59}$$

which means that $(\overline{c}_1, \overline{c}_2)$ and $(\underline{c}_1, \underline{c}_2)$ are coupled upper and lower solutions of system (6) (see Definition 2.2 in [32]).

Define two sequences of constant vectors $(\overline{c}_1^{(m)}, \overline{c}_2^{(m)})$ and $(\underline{c}_1^{(m)}, \underline{c}_2^{(m)})$, $m = 1, 2, \ldots$, as follows:

$$\begin{aligned} \overline{c}_1^{(m)} &= \overline{c}_1^{(m-1)} + \frac{1}{L}\overline{c}_1^{(m-1)}\left(1-\overline{c}_1^{(m-1)} - \frac{\underline{c}_2^{(m-1)}}{\left(\overline{c}_1^{(m-1)}\right)^2+\alpha}\right), \\ \overline{c}_2^{(m)} &= \overline{c}_2^{(m-1)} + \frac{\gamma}{L}\overline{c}_2^{(m-1)}\left(1-\frac{\overline{c}_2^{(m-1)}}{\beta\overline{c}_1^{(m-1)}}\right), \\ \underline{c}_1^{(m)} &= \underline{c}_1^{(m-1)} + \frac{1}{L}\underline{c}_1^{(m-1)}\left(1-\underline{c}_1^{(m-1)} - \frac{\overline{c}_2^{(m-1)}}{\left(\underline{c}_1^{(m-1)}\right)^2+\alpha}\right), \\ \underline{c}_2^{(m)} &= \underline{c}_2^{(m-1)} + \frac{\gamma}{L}\underline{c}_2^{(m-1)}\left(1-\frac{\underline{c}_2^{(m-1)}}{\beta\underline{c}_1^{(m-1)}}\right), \end{aligned} \tag{60}$$

where L is the Lipschitz constant for the vector field of system (6) when $(\underline{c}_1, \underline{c}_2) \leq (x, y) \leq (\overline{c}_1, \overline{c}_2)$.

Notice that the above two sequences of constant vectors are recursive sequences starting with $(\overline{c}_1^{(0)}, \overline{c}_2^{(0)}) = (\overline{c}_1, \overline{c}_2)$ and $(\underline{c}_1^{(0)}, \underline{c}_2^{(0)}) = (\underline{c}_1, \underline{c}_2)$. Then, by the principle of induction, the following monotone property of these sequences holds (see Lemma 2.1 in [33] for more details):

$$\begin{aligned} (0,0) < (\underline{c}_1, \underline{c}_2) &\leq \left(\underline{c}_1^{(m)}, \underline{c}_2^{(m)}\right) \leq \left(\underline{c}_1^{(m+1)}, \underline{c}_2^{(m+1)}\right) \leq \cdots \\ &\leq \left(\overline{c}_1^{(m+1)}, \overline{c}_2^{(m+1)}\right) \leq \left(\overline{c}_1^{(m)}, \overline{c}_2^{(m)}\right) \leq \cdots \leq (\overline{c}_1, \overline{c}_2). \end{aligned} \tag{61}$$

This monotone property implies that there exist positive constants $\overline{c}_i^* > 0$ and $\underline{c}_i^* > 0$ such that

$$\underline{c}_i \leq \underline{c}_i^{(m)} \leq \underline{c}_i^{(m+1)} \leq \underline{c}_i^* \leq \overline{c}_i^* \leq \overline{c}_i^{(m+1)} \leq \overline{c}_i^{(m)} \leq \overline{c}_i, \tag{62}$$

$$\lim_{m\to\infty} \overline{c}_i^{(m)} = \overline{c}_i^*, \quad \lim_{m\to\infty} \underline{c}_i^{(m)} = \underline{c}_i^*, \quad i = 1, 2. \tag{63}$$

By (60) and (63), we have

$$\begin{aligned} \overline{c}_1^*\left(1-\overline{c}_1^* - \frac{\underline{c}_2^*}{(\overline{c}_1^*)^2+\alpha}\right) &= 0, \qquad \gamma\overline{c}_2^*\left(1-\frac{\overline{c}_2^*}{\beta\overline{c}_1^*}\right) = 0, \\ \underline{c}_1^*\left(1-\underline{c}_1^* - \frac{\overline{c}_2^*}{(\underline{c}_1^*)^2+\alpha}\right) &= 0, \qquad \gamma\underline{c}_2^*\left(1-\frac{\underline{c}_2^*}{\beta\underline{c}_1^*}\right) = 0. \end{aligned} \tag{64}$$

From (64), it is easy to verify that

$$\begin{aligned} (1-\overline{c}_1^*)\left((\overline{c}_1^*)^2+\alpha\right) &= \beta\underline{c}_1^*, \\ (1-\underline{c}_1^*)\left((\underline{c}_1^*)^2+\alpha\right) &= \beta\overline{c}_1^*. \end{aligned} \tag{65}$$

Subtraction of these two equations gives

$$(\overline{c}_1^*)^2 - (\underline{c}_1^*)^2 + (\underline{c}_1^*)^3 - (\overline{c}_1^*)^3 + \alpha(\underline{c}_1^* - \overline{c}_1^*) = \beta(\underline{c}_1^* - \overline{c}_1^*). \tag{66}$$

Then we can prove $\overline{c}_1^* = \underline{c}_1^*$ by contradiction. In fact, if $\overline{c}_1^* \neq \underline{c}_1^*$, then (66) becomes

$$-(\overline{c}_1^* + \underline{c}_1^*) + (\underline{c}_1^*)^2 + (\overline{c}_1^*)^2 + \overline{c}_1^*\underline{c}_1^* + \alpha = \beta. \tag{67}$$

Equation (65) can be written as follows

$$\begin{aligned} (1-\overline{c}_1^*)\left((\overline{c}_1^*)^2+\alpha\right) + (1-\underline{c}_1^*)\beta &= \beta, \\ (1-\overline{c}_1^*)\beta + (1-\underline{c}_1^*)\left((\underline{c}_1^*)^2+\alpha\right) &= \beta. \end{aligned} \tag{68}$$

Solving (68) gives

$$\begin{aligned} 1-\overline{c}_1^* &= \frac{\beta\left((\underline{c}_1^*)^2+\alpha-\beta\right)}{\left((\overline{c}_1^*)^2+\alpha\right)\left((\underline{c}_1^*)^2+\alpha\right)-\beta^2}, \\ 1-\underline{c}_1^* &= \frac{\beta\left((\overline{c}_1^*)^2+\alpha-\beta\right)}{\left((\overline{c}_1^*)^2+\alpha\right)\left((\underline{c}_1^*)^2+\alpha\right)-\beta^2}. \end{aligned} \tag{69}$$

Substraction of the two equations of (69) and simplification lead to

$$\left((\overline{c}_1^*)^2+\alpha\right)\left((\underline{c}_1^*)^2+\alpha\right) - \beta^2 = \beta(\overline{c}_1^* + \underline{c}_1^*). \tag{70}$$

Addition of the two equations of (69) and using (70) yield

$$-(\overline{c}_1^* + \underline{c}_1^*) + (\underline{c}_1^*)^2 + (\overline{c}_1^*)^2 + \overline{c}_1^*\underline{c}_1^* = 2(\alpha-\beta). \tag{71}$$

It follows from (67) and (71) that

$$3(\alpha-\beta) = 0, \tag{72}$$

which is a contradiction under the assumption $\alpha > \beta$. So, the statement $\overline{c}_1^* = \underline{c}_1^*$ is proved.

By (64), we also have $\overline{c}_2^* = \beta\overline{c}_1^*$, $\underline{c}_2^* = \beta\underline{c}_1^*$. Therefore, $\overline{c}_2^* = \underline{c}_2^*$ since $\overline{c}_1^* = \underline{c}_1^*$. Letting $c_1^* = \overline{c}_1^* = \underline{c}_1^*$ and $c_2^* = \overline{c}_2^* = \underline{c}_2^*$, then (c_1^*, c_2^*) is the positive solution of (8). In addition, notice that when $\alpha > \beta$, (8) has the unique positive solution (x^*, y^*). Thus, $(c_1^*, c_2^*) = (x^*, y^*)$. Then from the result due to Pao (see Theorem 2.2 in [33]), the proof of Theorem is complete. □

3.3. Direction and Stability of Hopf Bifurcation Associated with the Critical Values of Delay. In Section 3.1, we have shown that the system (6) undergoes the Hopf bifurcation at critical values $\tau = \tau_j$. In this subsection, we will derive the direction of the Hopf bifurcation and stability of the bifurcating periodic orbits from the interior equilibrium E^* of system (6) at $\tau = \tau_j$. We will employ the algorithm of Faria and Magalhães [34] to compute explicitly the normal forms of system (6) on the center manifold.

We rescale the time by $t \mapsto t/\tau$ to normalize the delay and then introduce the new parameter $\mu = \tau - \tau_j$ so that $\mu = 0$ is the critical value of Hopf singularity. System (30) can be rewritten as

$$\dot{z}(t) = L(\mu) z_t + F(z_t, \mu), \tag{73}$$

in the phase space $C = C([-1, 0], \mathbb{R}^2)$, where for $\varphi = (\varphi_1, \varphi_2)^T \in C$, we have

$$L(\mu)(\varphi) = (\tau_j + \mu)\begin{pmatrix} -r_1\varphi_1(0) - r_2\varphi_2(-1) \\ \gamma\beta\varphi_1(0) - \gamma\varphi_2(0) \end{pmatrix},$$
$$F(\varphi, \mu) = (\tau_j + \mu)\begin{pmatrix} \sum_{i+j\geq 2} \frac{1}{i!\,j!} f_{ij}^{(1)} \varphi_1^i(0)\,\varphi_2^j(-1) \\ \sum_{i+j\geq 2} \frac{1}{i!\,j!} f_{ij}^{(2)} \varphi_1^i(0)\,\varphi_2^j(0) \end{pmatrix}. \tag{74}$$

By the Riesz representation theorem, there exists a function $\eta : [-1, 0] \to \mathbb{R}^2 \times \mathbb{R}^2$ of bounded variation such that

$$L(\mu)\varphi = \int_{-1}^{0} \left[d\eta_\mu(\theta)\right] \varphi(\theta). \tag{75}$$

Setting $\omega_* = \omega_0\tau_j$, then $\Lambda_0 = \{i\omega_*, -i\omega_*\}$ and $B = \mathrm{diag}\{i\omega_*, -i\omega_*\}$. Let P be the generalized eigenspace associated with the eigenvalues in Λ_0 and let P^* be its dual space. For $\mathbb{R}^{2*}$, the 2-dimensional space of row vectors, define $C^* = C([0, 1]; \mathbb{R}^{2*})$ and the adjoint bilinear form on $C^* \times C$ as follows:

$$\langle \psi(s), \phi(\theta) \rangle = \psi(0)\phi(0) - \int_{-1}^{0} \int_{0}^{\theta} \psi(\xi - \theta)\, d\eta_\mu(\theta)\, \phi(\xi)\, d\xi, \tag{76}$$
$$\psi(s) \in C^*,\ \phi(\theta) \in C.$$

Denote the dual bases of P and P^* by Φ and Ψ, respectively. Consider $\Phi = (\phi_1, \phi_2)$ with

$$\phi_1(\theta) = e^{i\omega_*\theta} v, \qquad \phi_2(\theta) = e^{-i\omega_*\theta}\overline{v}, \tag{77}$$

where v is a nonzero solution in $\mathbb{C}^2$ to the following equation:

$$L_0\left(e^{i\omega_* \cdot} I\right) v = i\omega_* v, \tag{78}$$

and choose a basis Ψ for the adjoint space P^* such that $\langle \Psi, \Phi \rangle = I_2$, where I_2 is a 2×2 identical matrix. So $\Psi(s) = \mathrm{col}(\psi_1(s), \psi_2(s))$ with

$$\psi_1(s) = e^{-i\omega_* s} u^T, \quad \psi_2(s) = e^{i\omega_* s}\overline{u}^T, \quad 0 \leq s \leq 1, \tag{79}$$

where $u^T \in \mathbb{C}^2$ is the solution to the equation

$$u^T L_0\left(e^{i\omega_* \cdot} I\right) = i\omega_* u^T. \tag{80}$$

and satisfies $\langle \psi_1(s), \phi_1(\theta) \rangle = 1$. By direct computation, we can choose

$$v = \begin{pmatrix} v_1 \\ v_2 \end{pmatrix} = \begin{pmatrix} 1 \\ -\dfrac{r_1 + i\omega_0}{r_2 e^{-i\omega_*}} \end{pmatrix},$$
$$u = \begin{pmatrix} u_1 \\ u_2 \end{pmatrix} = d\begin{pmatrix} -\dfrac{\gamma + i\omega_0}{r_2 e^{-i\omega_*}} \\ 1 \end{pmatrix}, \tag{81}$$

where $d = -r_2 e^{-i\omega_*}/(r_1 + \gamma + 2i\omega_0 + r_1\gamma\tau_j + (r_1 + \gamma)i\omega_* - \omega_0\omega_*)$.

Following the normal form theory of functional differential equations due to Faria and Magalhães [34] and using a very similar procedure as in [29] but a tedious calculation, we can obtain the following normal form at the critical values τ_j:

$$\dot{w} = Bw + \begin{pmatrix} A_1 w_1 \mu \\ \overline{A}_1 w_2 \mu \end{pmatrix} + \begin{pmatrix} A_2 w_1^2 w_2 \\ \overline{A}_2 w_1 w_2^2 \end{pmatrix} + O\left(|w|\,\mu^2 + |w^4|\right), \tag{82}$$

where $w = (w_1, w_2)^T \in \mathbb{C}^2$. The coefficients A_1 and A_2 can be determined as follows:

$$A_1 = i\omega_0 u^T v,$$
$$A_2 = \frac{i}{2\omega_*}\left(a_{20}a_{11} - 2|a_{11}|^2 - \frac{1}{3}|a_{02}|^2\right) + \frac{1}{2}(a_{21} + b_{21}), \tag{83}$$

where

$$a_{20} = \tau_j(b_1 u_1 + b_2 u_2), \qquad a_{11} = \tau_j(b_3 u_1 + b_4 u_2),$$
$$a_{02} = \tau_j\left(\overline{b}_1 u_1 + \overline{b}_2 u_2\right) \tag{84}$$

with

$$b_1 = f_{20}^{(1)} v_1^2 + 2f_{11}^{(1)} v_1 v_2 e^{-i\omega_*},$$
$$b_2 = f_{20}^{(2)} v_1^2 + 2f_{11}^{(2)} v_1 v_2 + f_{02}^{(2)} v_2^2,$$
$$b_3 = f_{20}^{(1)}|v_1|^2 + 2f_{11}^{(1)}\,\mathrm{Re}\left\{v_1\overline{v}_2 e^{i\omega_*}\right\},$$
$$b_4 = f_{20}^{(2)}|v_1|^2 + 2f_{11}^{(2)}\,\mathrm{Re}\{v_1\overline{v}_2\} + f_{02}^{(2)}|v_2|^2,$$
$$a_{21} = \tau_j u_1\left(f_{30}^{(1)} v_1|v_1|^2 + f_{21}^{(1)}\left(v_1^2\overline{v}_2 e^{i\omega_*} + 2|v_1|^2 v_2 e^{-i\omega_*}\right)\right) + \tau_j u_2\left(f_{30}^{(2)} v_1|v_1|^2 + f_{21}^{(2)}\left(v_1^2\overline{v}_2 + 2|v_1|^2 v_2\right) + f_{12}^{(2)}\left(v_2^2\overline{v}_1 + 2|v_2|^2 v_1\right)\right),$$
$$b_{21} = \tau_j u^T \times \begin{pmatrix} d_1 h_{11}^{(1)}(0) + \overline{d}_1 h_{20}^{(1)}(0) + d_2 h_{11}^{(2)}(-1) + \overline{d}_2 h_{20}^{(2)}(-1) \\ d_3 h_{11}^{(1)}(0) + \overline{d}_3 h_{20}^{(1)}(0) + d_4 h_{11}^{(2)}(0) + \overline{d}_4 h_{20}^{(2)}(0) \end{pmatrix} \tag{85}$$

with

$$d_1 = f_{20}^{(1)}\nu_1 + f_{11}^{(1)}\nu_2 e^{-i\omega_*}, \qquad d_2 = f_{11}^{(1)}\nu_1,$$
$$d_3 = f_{20}^{(2)}\nu_1 + f_{11}^{(2)}\nu_2, \qquad d_4 = f_{11}^{(2)}\nu_1 + f_{02}^{(2)}\nu_2,$$

$$h_{20}(\theta) = -\frac{1}{i\omega_*}\left(a_{20}e^{i\omega_*\theta}\nu + \frac{1}{3}\overline{a}_{02}e^{-i\omega_*\theta}\overline{\nu}\right) + e^{2i\omega_*\theta}\begin{pmatrix} \dfrac{b_1(2i\omega_0+\gamma) - b_2 r_2 e^{-2i\omega_*}}{(2i\omega_0+\gamma)(2i\omega_0+r_1) + \beta r_2\gamma e^{-2i\omega_*}} \\ \dfrac{\beta\gamma b_1 + b_2(2i\omega_0+r_1)}{(2i\omega_0+\gamma)(2i\omega_0+r_1) + \beta r_2\gamma e^{-2i\omega_*}} \end{pmatrix},$$

$$h_{11}(\theta) = \frac{2}{i\omega_*}\left(a_{11}e^{i\omega_*\theta}\nu - \overline{a}_{11}e^{-i\omega_*\theta}\overline{\nu}\right) + \begin{pmatrix} \dfrac{2\gamma b_3 - 2r_2 b_4}{\gamma(r_1+r_2\beta)} \\ \dfrac{2\beta\gamma b_3 + 2r_1 b_4}{\gamma(r_1+r_2\beta)} \end{pmatrix}. \tag{86}$$

The normal form (82) can be written in real coordinates $\widetilde{w} = (\widetilde{w}_1, \widetilde{w}_2)^2 \in \mathbb{R}^2$ through the change of variables $\widetilde{w}_1 = w_1 - iw_2$, $\widetilde{w}_2 = w_1 + iw_2$. Transforming to polar coordinates $\widetilde{w}_1 = \rho\cos\xi$, $\widetilde{w}_2 = \rho\sin\xi$, the normal form becomes

$$\dot{\rho} = K_1\mu\rho + K_2\rho^3 + O\left(\mu^2\rho + \left|(\rho, x)\right|^4\right),$$
$$\dot{\xi} = -\omega_* + O\left(\left|(\rho,\mu)\right|\right) \tag{87}$$

with $K_1 = \operatorname{Re} A_1$, $K_2 = \operatorname{Re} A_2$. It is well known [35] that the sign of K_1K_2 determines the direction of the bifurcation (supercritical if $K_1K_2 < 0$, subcritical if $K_1K_2 > 0$), and the sign of K_2 determines the stability of the nontrivial periodic orbits (stable if $K_2 < 0$, unstable if $K_2 > 0$). Thus, if the coefficients of system (4) are given, then we will analyze the direction of the Hopf bifurcation and stability of the bifurcating periodic orbits at $\tau = \tau_j$.

4. Numerical Simulations

In this section, we present some numerical simulations to verify and extend our theoretical analysis proved in Section 3 by using the Simulink for Matlab. To investigate the effect of delay, we are interested in the cases when $(\alpha, \beta) \in D_{11}$, $(\alpha, \beta) \in D_2$, and $(\alpha, \beta) \in D_3$. We would also like to mention that for the case of delay, the initial values should be given by $x(t) = \varphi_1(t)$, $y(t) = \varphi_2(t)$ for $t \in [-\tau, 0]$. However, in the Simulink for Matlab, we only need to specify the initial values as $x(0)$ and $y(0)$. The initial values for the case of delay can be selected automatically by the default function of Simulink.

(i) Taking $\alpha = 0.2$ and $\beta = 2$ such that $(\alpha, \beta) \in D_{11}$, system (6) has a unique positive equilibrium $E^*(0.0946, 0.1892)$. Without delay, the positive equilibrium E^* is asymptotically stable for any $\gamma > 0$. Let $\gamma = 0.2$ and then by (39), we have the critical value $\tau_0 \doteq 1.2508$ of delay and it follows from Theorem 4 that E^* is asymptotically stable for $0 \le \tau < \tau_0 \doteq 1.2508$ and unstable for $\tau > \tau_0 \doteq 1.2508$, as shown in Figures 4(a) and 4(b) for $\tau = 0.5$. Furthermore, by the procedure of Section 3.3, we get $K_1 \doteq 0.0882 > 0$, and $K_2 \doteq 5.2428 > 0$, which implies that the Hopf bifurcation associated with this critical value $\tau_0 \doteq 1.2508$ is subcritical. So, there exists a sufficiently small positive real number ε_0 such that for each $\tau \in (\tau_0 - \varepsilon_0, \tau_0)$, system (6) has an unstable periodic solution near the positive equilibrium $E^*(0.0946, 0.1892)$. Taking $\tau = 1.15 < \tau_0$, Figures 4(c) and 4(d) show the existence of the subcritical Hopf bifurcation. In this case, a small-amplitude unstable periodic solution, coming from the Hopf bifurcation, and a large-amplitude stable periodic solution coexist. Taking $\tau = 1.3 > \tau_0$, the positive equilibrium E^* becomes unstable and numerical simulation also shows the existence of large-amplitude stable periodic solution (see Figures 4(e) and 4(f)).

(ii) Taking $\alpha = 0.2$ and $\beta = 1.2$ such that $(\alpha, \beta) \in D_2$, system (6) has a unique positive equilibrium $E^*(0.1578, 0.1894)$. Without delay, the parameter γ affects the stability of the positive equilibrium E^*. By Lemma 2, we get $\gamma_0 \doteq 0.0287$. The positive equilibrium E^* is stable for $\gamma > \gamma_0$, and unstable for $\gamma < \gamma_0$ and system (7) undergoes Hopf bifurcation near the positive equilibrium E^* at $\gamma = \gamma_0$. By (28), we have $a_3(\gamma_0) = 0.3822 > 0$, which means that the Hopf bifurcation occurring at γ_0 is subcritical. So, there exists a sufficiently small positive real number ε_1 such that for any $\gamma \in (\gamma_0, \gamma_0 + \varepsilon_1)$, system (7) has an unstable periodic orbit near the positive equilibrium E^*. Taking $\gamma = 0.02 < \gamma_0$, Figures 5(a) and 5(b) illustrate the instability of the positive equilibrium E^* and the existence of a large-amplitude stable periodic orbit. Taking $\gamma = 0.04$ larger than and closer to γ_0, Figures 5(c) and 5(d) illustrate the stability of the positive equilibrium E^* and the existence of subcritical Hopf bifurcation. In this case, a small-amplitude unstable periodic solution, coming from the Hopf bifurcation, and a large-amplitude stable periodic solution coexist. Taking $\gamma = 0.06$ larger than and away from γ_0, the positive equilibrium E^* is stable and there are no Hopf bifurcating periodic orbits, as shown in Figures 5(e) and 5(f).

To investigate the effect of delay, we fix α, β, and γ. For $(\alpha, \beta) = (0.2, 1.2) \in D_2$ and $\gamma = 0.04 \in (\gamma_0, \gamma_0 + \varepsilon_1)$, the positive equilibrium $E^*(0.1578, 0.1894)$ is stable and there exists an unstable periodic orbit near the positive equilibrium E^* (see Figures 5(c) and 5(d)). The stability of the positive equilibrium E^* changes with the increase of delay. By (39), the critical value of delay is $\tau_0 \doteq 0.3346$. By the procedure of Section 3.3, we have $K_1 = 0.0056$, and $K_2 = 1.1923$, which implies that the Hopf bifurcation occurring at $\tau_0 \doteq 0.3346$ is subcritical. So, the positive equilibrium E^* is stable with the coexistence of small-amplitude stable and large-amplitude stable periodic orbits for $0 \le \tau < \tau_0 \doteq 0.3346$ and unstable for $\tau > \tau_0 \doteq 0.3346$. Figures 6(a) and 6(b) and Figures 6(c) and 6(d) are numerical simulations for $\tau = 0.2 \in [0, \tau_0)$ and $\tau = 0.4 > \tau_0$, respectively. For $(\alpha, \beta) = (0.2, 1.2) \in D_2$ and $\gamma = 0.06 > \gamma_0 + \varepsilon_1$, the positive equilibrium $E^*(0.1578, 0.1894)$ is stable and there are no periodic orbits near the positive equilibrium E^* (see Figures 5(e) and 5(f)). In this case, the critical value of delay is $\tau_0 \doteq 0.6207$. The positive equilibrium E^* is stable for $0 \le \tau < \tau_0 \doteq 0.6207$ and unstable for

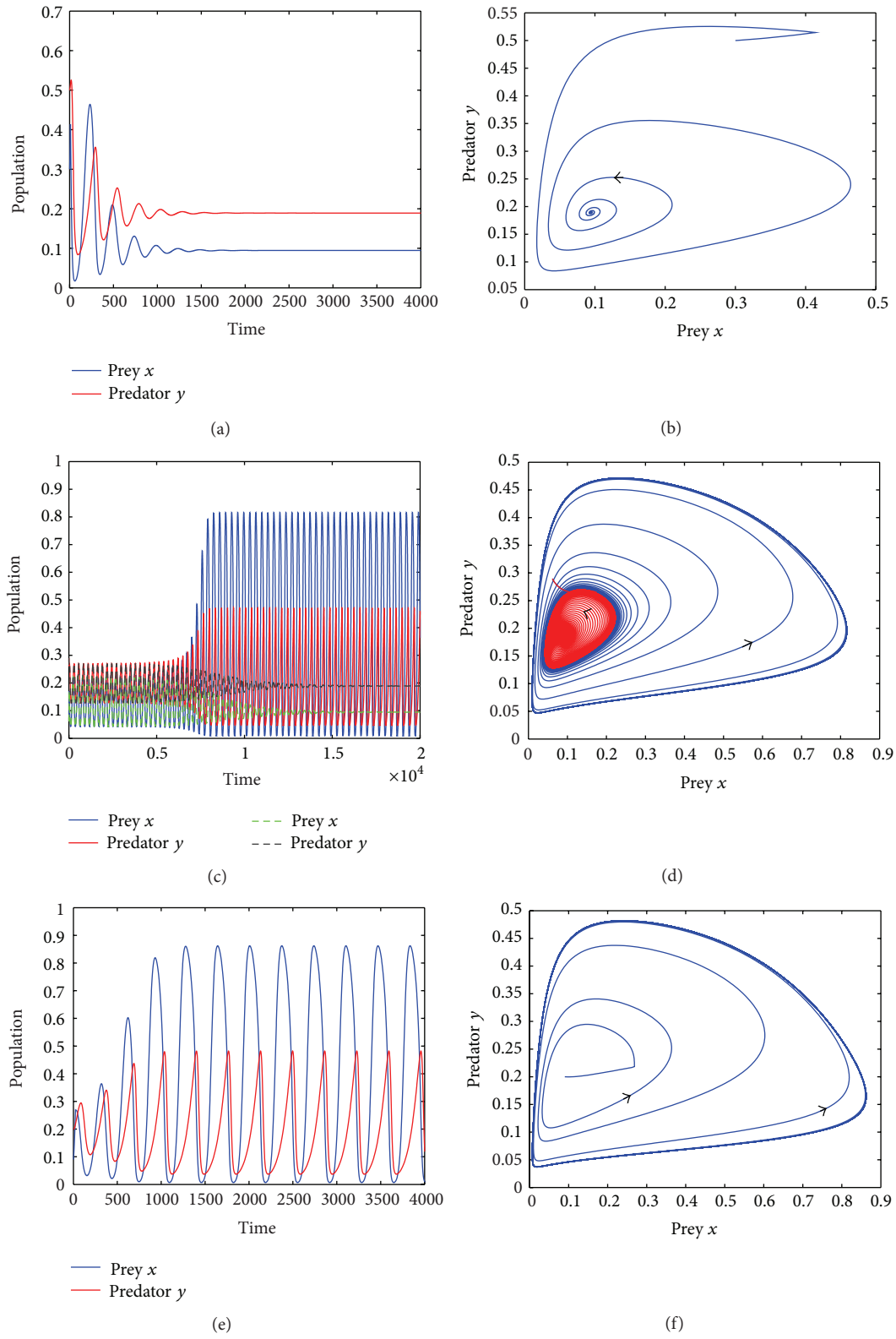

FIGURE 4: The trajectory graphs and phase portrait of system (6) for $(\alpha, \beta) \in D_{11}$ with $\alpha = 0.2$, $\beta = 2$, and $\gamma = 0.2$. (a)-(b) When $0 \leq \tau < \tau_0$, the equilibrium E^* is stable. (c)-(d) Simulations of subcritical Hopf bifurcation. Starting from the initial value $(x(0), y(0)) = (0.0615, 0.2897)$, the trajectory slowly gets away from a small-amplitude unstable periodic solution and finally converges to a large-amplitude stable periodic solution. Starting from the initial value $(x(0), y(0)) = (0.0615, 0.2895)$, the trajectory converges to E^*. (e)-(f) When $\tau > \tau_0$, the equilibrium E^* is unstable with a large-amplitude stable periodic solution.

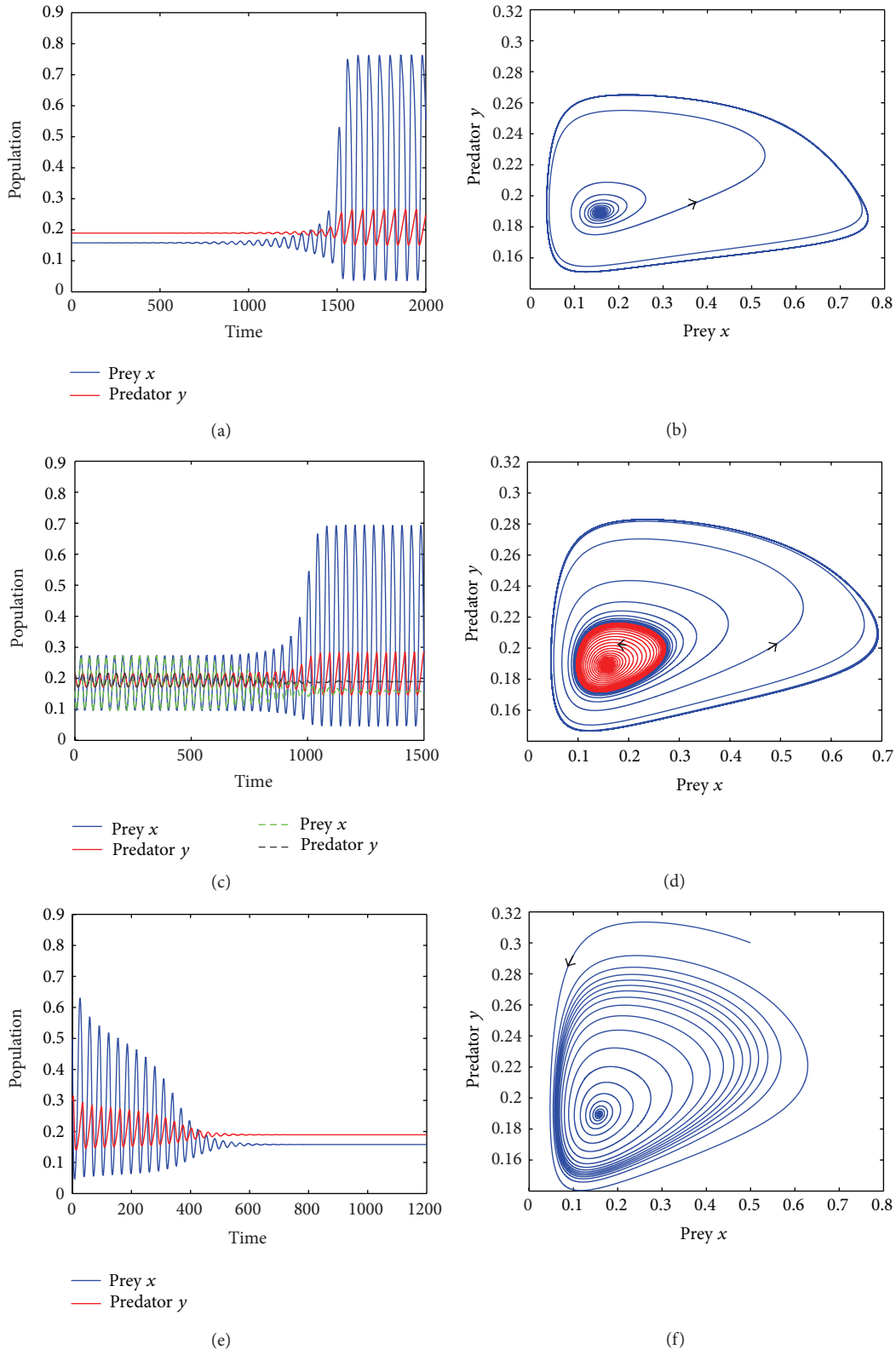

FIGURE 5: The trajectory graphs and phase portrait of system (7) without delay for $(\alpha, \beta) \in D_2$ with $\alpha = 0.2$ and $\beta = 1.2$. (a)-(b) $\gamma = 0.02 < \gamma_0$. The positive equilibrium E^* is unstable with a large-amplitude stable periodic orbit. The initial value is $(0.1578, 0.18935)$. (c)-(d) $\gamma = 0.04 > \gamma_0$. The positive equilibrium E^* is stable, and a small-amplitude unstable periodic solution and a large-amplitude stable periodic solution coexist. The initial values are $(0.1578, 0.21532)$ and $(0.1578, 0.21533)$. (e)-(f) $\gamma = 0.06 > \gamma_0$. The positive equilibrium E^* is stable and there are no Hopf bifurcating periodic orbits. The initial value is $(0.5, 0.3)$.

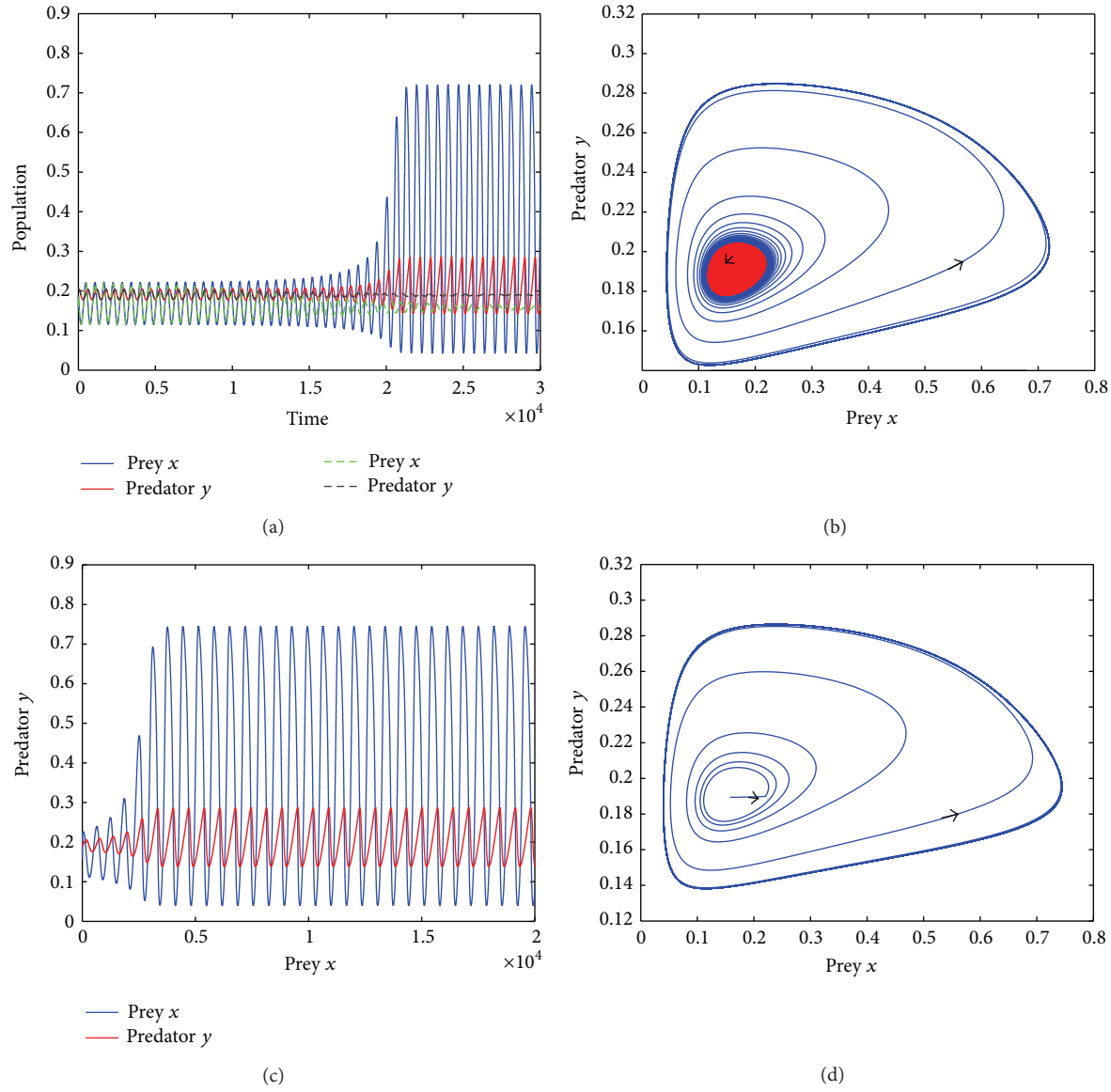

FIGURE 6: The trajectory graphs and phase portrait of system (6) for $(\alpha, \beta) \in D_2$ with $\alpha = 0.2$, $\beta = 1.2$, and $\gamma = 0.04$. (a)-(b) For $\tau = 0.2 \in [0, \tau_0)$, the positive equilibrium E^* is stable with small-amplitude unstable and large-amplitude stable periodic orbits. The initial values are $(0.1578, 0.21532)$ and $(0.1578, 0.21533)$. (c)-(d) For $\tau = 0.4 > \tau_0$, the positive equilibrium E^* is unstable with a large-amplitude stable periodic orbit. The initial value is $(0.1578, 0.18935)$.

$\tau > \tau_0 \doteq 0.6207$. Figures 7(a) and 7(b), Figures 7(c) and 7(d), and Figures 7(e) and 7(f) are numerical simulations for $\tau = 0.04 < \tau_0 \doteq 0.6207$, $\tau = 0.05 < \tau_0 \doteq 0.6207$, and $\tau = 0.65 > \tau_0 \doteq 0.6207$, respectively. It follows from the procedure of Section 3.3 that $K_1 = 0.0154$ and $K_2 = 2.1776$, which implies that the Hopf bifurcation occurring at $\tau_0 \doteq 0.6207$ is also subcritical. Thus, there exists a positive real number ε_2 such that for each $\tau \in (\tau_0 - \varepsilon_2, \tau_0)$, there exists an unstable periodic orbit, as shown in Figures 7(c) and 7(d). For $\tau > \tau_0 \doteq 0.6207$, the the positive equilibrium E^* becomes unstable and there exists a large-amplitude stable periodic orbit, as shown in Figures 7(e) and 7(f) for $\tau = 0.65 > \tau_0$.

(iii) Taking $\alpha = 0.01$ and $\beta = 0.24$ such that $(\alpha, \beta) \in D_3$, system (6) has three positive equilibria $E_1^*(0.0492, 0.0118)$, $E_2^*(0.3244, 0.0779)$, and $E_3^*(0.6264, 0.1503)$. The positive equilibrium E_2^* is always unstable for any $\gamma > 0$ and $\tau \geq 0$. But the parameters γ and τ affect the stability of E_1^* and E_3^*. Without delay, the critical values of γ for E_1^* and E_3^* are $\gamma_{01} = 0.3215$ and $\gamma_{03} = 0.1024$. The positive equilibrium E_1^* (resp., E_3^*) is asymptotically stable for $\gamma > \gamma_{01}$ (resp., $\gamma > \gamma_{03}$) and unstable for $\gamma < \gamma_{01}$ (resp., $\gamma < \gamma_{03}$). Taking $\gamma = 0.1 < \min\{\gamma_{01}, \gamma_{03}\}$, all of these three equilibria are unstable. There is a large-amplitude stable periodic orbit enclosing these three equilibria, as shown in Figures 8(a) and (b). For $\gamma_{03} < \gamma < \gamma_{01}$, the positive equilibria E_1^* and E_2^* are still unstable, but the positive equilibrium E_3^* becomes stable, as shown in Figures 8(c) and 8(d) with $\gamma = 0.3$.

When $\gamma > \max\{\gamma_{01}, \gamma_{03}\}$, the positive equilibria E_1^* and E_3^* both become asymptotically stable. Taking $\gamma = 0.5$, Figures 9(a) and 9(b) illustrate this theoretical result. The critical

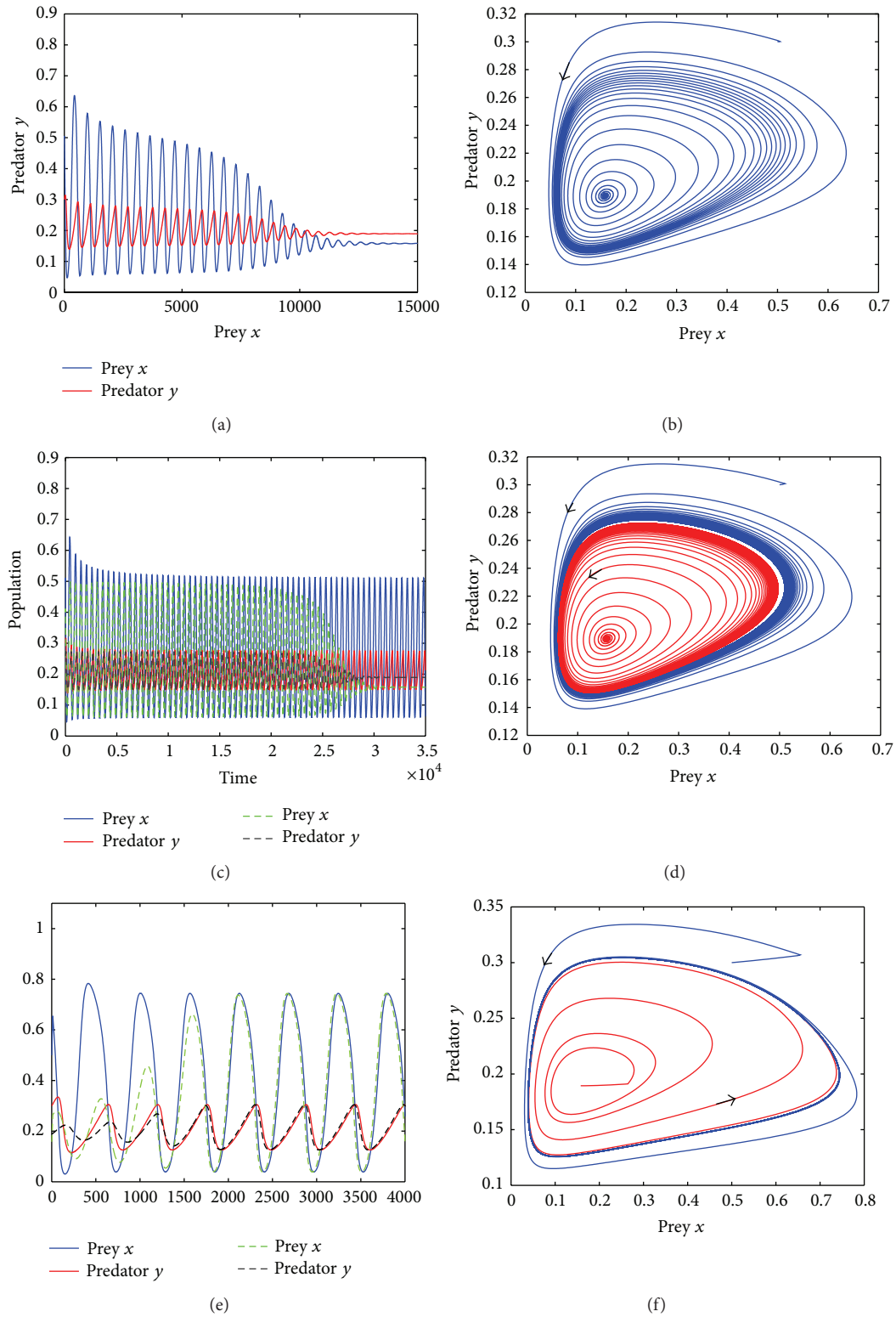

FIGURE 7: The trajectory graphs and phase portrait of system (6) for $(\alpha, \beta) \in D_2$ with $\alpha = 0.2$, $\beta = 1.2$, and $\gamma = 0.06$. (a)-(b) For $\tau = 0.04 < \tau_0$, the positive equilibrium E^* is stable. The initial values are $(0.5, 0.3)$. (c)-(d) For $\tau = 0.05 < \tau_0$, the positive equilibrium E^* is stable with an unstable periodic orbit. The initial values are $(0.4, 0.258)$ and $(0.5, 0.3)$. (e)-(f) For $\tau = 0.65 > \tau_0$, the positive equilibrium E^* is unstable with an stable periodic orbit. The initial values are $(0.1578, 0.18935)$ and $(0.5, 0.3)$.

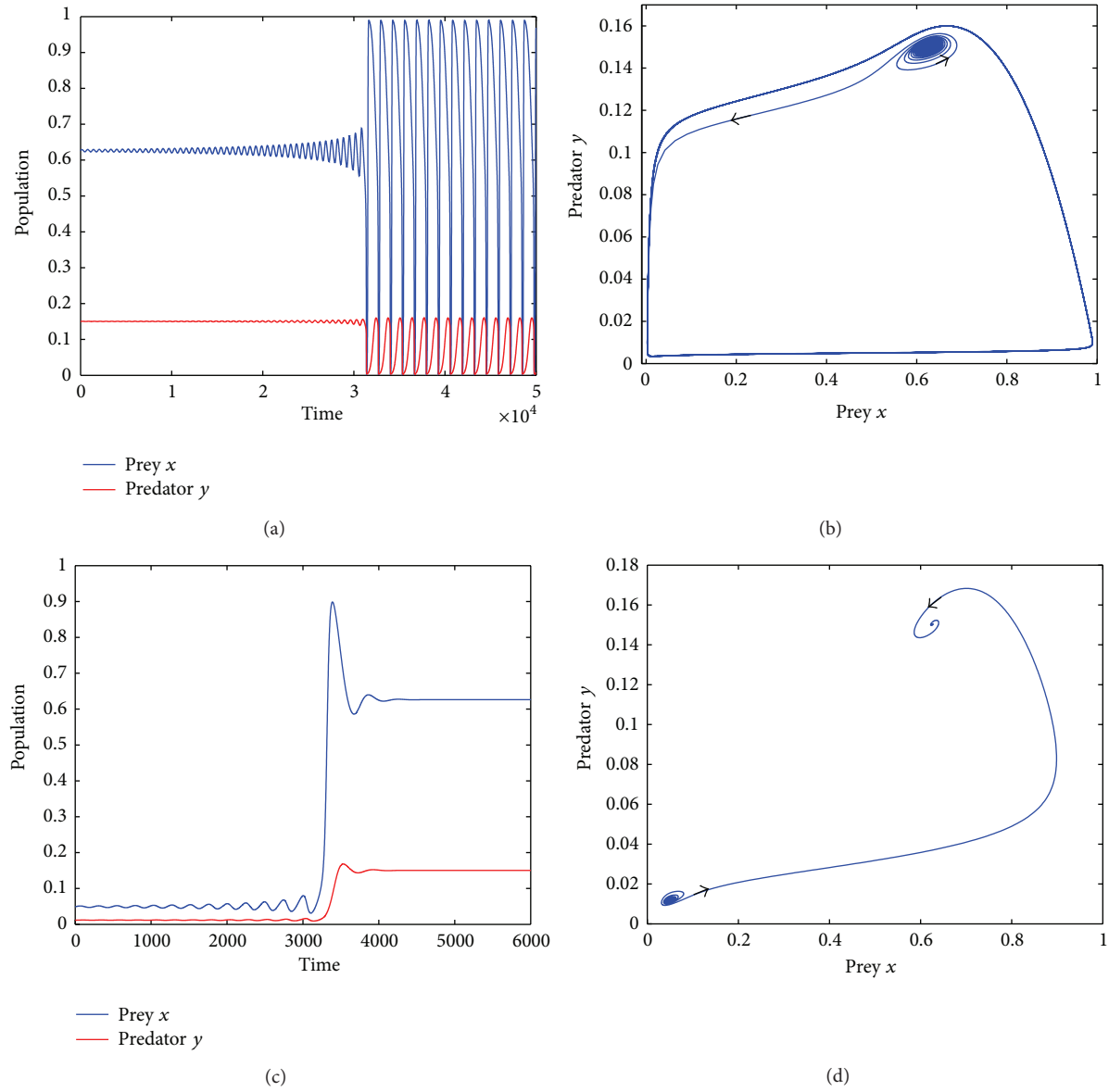

FIGURE 8: The trajectory graphs and phase portrait of system (7) without delay for $(\alpha, \beta) \in D_3$ with $\alpha = 0.01$ and $\beta = 0.24$. (a)-(b) $\gamma = 0.1 < \min\{\gamma_{01}, \gamma_{03}\}$. The initial value is $(0.626, 0.15)$. All of the three equilibria are unstable and there exists a stable periodic orbit. (c)-(d) $\gamma_{03} < \gamma = 0.3 < \gamma_{01}$. The initial value is $(0.049, 0.0116)$. The positive equilibria E_1^* and E_2^* are unstable and the positive equilibrium E_3^* is stable.

values of the delay for these two positive equilibria E_1^* and E_3^* are $\tau_{01} \doteq 0.3782$ and $\tau_{03} \doteq 2.3129$, respectively. Thus the positive equilibrium E_1^* is asymptotically stable for $\tau < \tau_{01}$ and unstable for $\tau > \tau_{01}$, and the positive equilibrium E_3^* is asymptotically stable for $\tau < \tau_{03}$ and unstable for $\tau > \tau_{03}$. According to the procedure of Section 3.3, we obtain that $K_1 \doteq 0.0851 > 0$, and $K_2 \doteq 49.9838 > 0$ for E_1^* and τ_{01}, and $K_1 \doteq 0.1197 > 0$, and $K_2 \doteq 13.9616 > 0$ for E_3^* and τ_{03}. So, the delay-induced Hopf bifurcations for these two positive equilibria are both subcritical. Taking $\tau = 0.37 < \min\{\tau_{01}, \tau_{03}\}$, the positive equilibrium E_1^* and E_3^* are both asymptotically stable. Near the positive equilibria E_1^*, the subcritical Hopf bifurcation occurs. Figures 9(c) and 9(d) illustrate the existence of this subcritical Hopf bifurcation and show that there is an orbit connecting the unstable periodic orbit to the stable equilibrium E_3^*. When $\tau > \max\{\tau_{01}, \tau_{03}\}$, the positive equilibria E_1^* and E_3^* both becomes unstable. There is a large-amplitude stable periodic orbit enclosing the three equilibria, as shown in Figures 9(e) and 9(f) for $\tau = 2.5$.

5. Conclusions

In this paper, we have considered a predator-prey system with the hunting delay. By analysing the concerned characteristic equations, local asymptotic stability of the various positive equilibria of the system with or without delay is discussed. The dynamics of the system can be described in the plane of the parameters α and β. For the system without delay, the bistability (existence of two stable equilibria) occurs in some parameter regions. We have shown that the ratio ($\gamma = s/r$) of

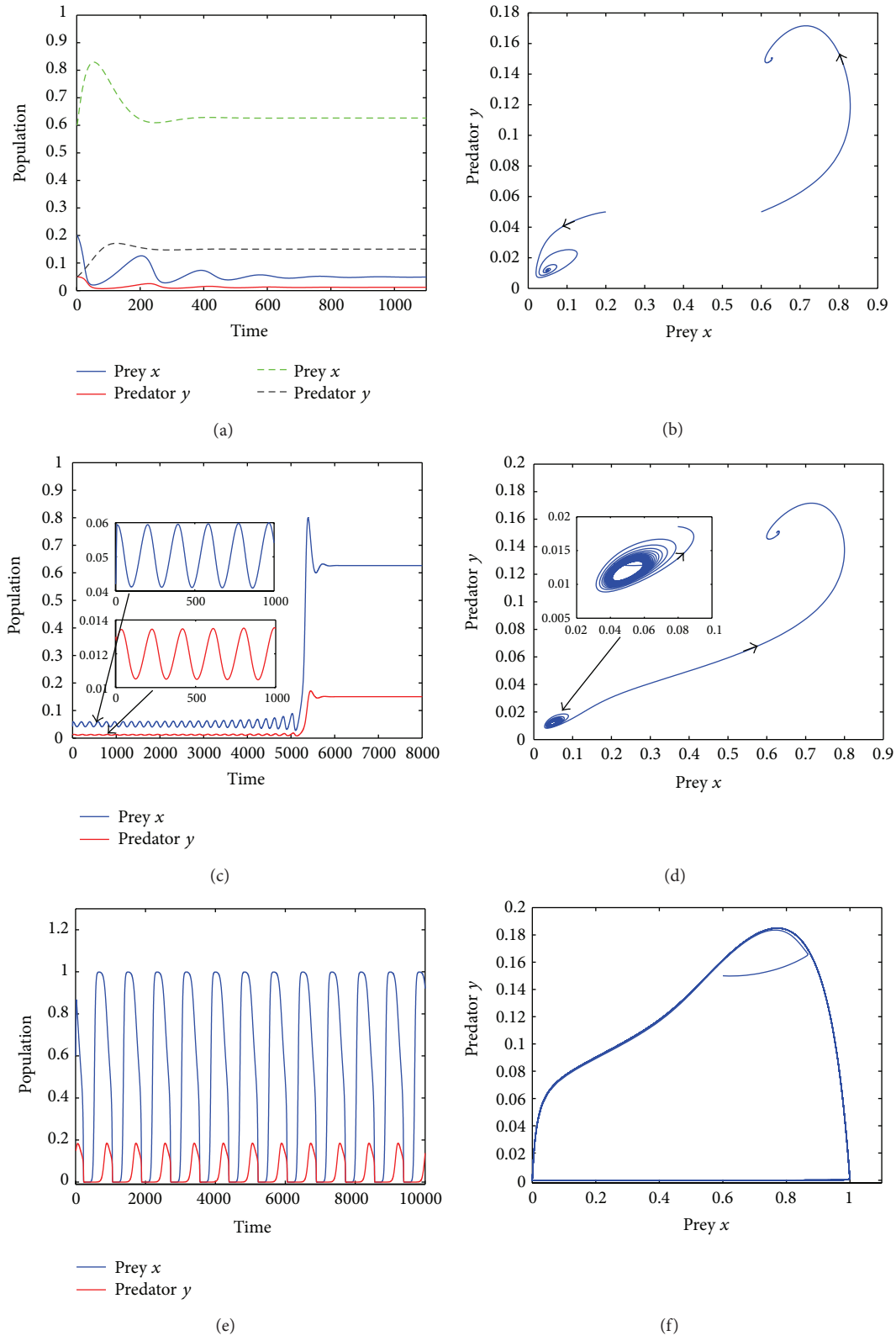

FIGURE 9: The trajectory graphs and phase portrait of system (6) for $(\alpha, \beta) \in D_3$ with $\alpha = 0.01$, $\beta = 0.24$, and $\gamma = 0.5$. (a)-(b) When $\tau = 0$, the positive equilibria E_1^* and E_3^* are both asymptotically stable. The initial values are $(0.2, 0.05)$ and $(0.6, 0.05)$. (c)-(d) When $\tau = 0.37 < \min\{\tau_{01}, \tau_{03}\}$, the positive equilibria E_1^* and E_3^* are both asymptotically stable and there exists a subcritical Hopf bifurcation near E_1^*. Here, the initial values is $(0.042, 0.013)$. (e)-(f) When $\tau = 2.5 > \max\{\tau_{01}, \tau_{03}\}$. All of the three equilibria become unstable and there exists a large-amplitude stable periodic orbit enclosing the three equilibria. Here, the initial value is $(0.6, 0.15)$.

the intrinsic growth rates of the predator and prey is the key parameter which has an important influence on the dynamics of the system. In the region where the system has only one positive equilibrium and the ratio γ can affect the stability of this positive, the ratio γ can induce large-amplitude periodic oscillations of both species and there are two limit cycles (one is stable and the other is unstable) near the critical value of the ratio via subcritical Hopf bifurcation. In the region where the system has three positive equilibria, the dynamics of the system can evolve from a heteroclinic orbit connecting one positive equilibrium to a large-amplitude limit cycle enclosing three equilibria (see Figures 8(a) and 8(b)), a heteroclinic orbit connecting two equilibria (see Figures 8(c) and 8(d)), two stable equilibria with the increase of the ratio γ (see Figures 9(a) and 9(b)).

When the hunting delay is introduced by the system, its effect on the dynamics of all positive equilibria is investigated. We first show that when $\alpha < \beta$ (or equivalent to $kmn < ar$), the unique positive equilibrium is global stability for any nonnegative hunting delay. Then the absolute investigate the influence of the delay on the local stability of the positive equilibria. For the case when the system has the unique positive equilibrium, depending on the choice of the parameters α and β, the delay can induce the emergence of two limit cycles with one stable subcritical Hopf bifraction and another unstable subcritical Hopf bifurcation (see Figures 4(c) and 4(d)) and induce the emerge of semistable limit cycle which is inward unstable and outward stable (see Figures 7(c) and 7(d)). For the case when the system has the three positive equilibria, delay can induce a heteroclinic orbit connecting a limit cycle to a stable equilibrium (see Figures 9(c) and 9(d)). The analytical expressions that determine the properties of bifurcating periodic solutions are also obtained by using the normal form theory and the centre manifold theorem. It is also worthy to mention that for the case without delay, the size of limit cycle increases with the decreasing magnitude of the ratio of the intrinsic growth rates of the predator and prey, but for the case with delay, the size of limit cycle increases with the increasing magnitude of the hunting delay.

Acknowledgments

The authors would like to thank the three anonymous referees very much for their constructive comments, which resulted in much improvement of the paper. The authors would also like to express appreciation for the support from the National Natural Science Foundation of China (nos. 11201294 and 11032009), the Scientific Research Foundation for the Returned Overseas Chinese Scholars, the Fundamental Research Funds for the Central Universities, and the Program for New Century Excellent Talents in University (NCET-11-0385).

References

[1] S. Allesina and S. Tang, "Stability criteria for complex ecosystems," *Nature*, vol. 483, no. 7388, pp. 205–208, 2012.

[2] A. J. Lotka, "Analytical note on certain rhythmic relations in organic systems," *Proceedings of the National Academy of Sciences of the United States of America*, vol. 6, no. 7, pp. 410–415, 1920.

[3] V. Volterra, "Variations and uctuations of the number of individuals in animal species living together," in *Animal Ecology*, R. N. Chapman, Ed., McGraw-Hill, New York, NY, USA, 1931.

[4] C. S. Holling, "The components of predation as revealed by a study of small mammal predation of the European pine sawfly," *The Canadian Entomologist*, vol. 91, no. 5, pp. 293–320, 1959.

[5] C. S. Holling, "Some characteristics of simple types of predation and parasitism," *The Canadian Entomologist*, vol. 91, no. 6, pp. 385–398, 1959.

[6] C. S. Holling, "The functional response of predators to prey density and its role in mimicry and population regulation," *Memoirs of the Entomological Society of Canada*, vol. 46, pp. 1–60, 1965.

[7] P. H. Leslie, "Some further notes on the use of matrices in population mathematics," *Biometrika*, vol. 35, pp. 213–245, 1948.

[8] P. H. Leslie, "A stochastic model for studying the properties of certain biological systems by numerical methods," *Biometrika*, vol. 45, pp. 16–31, 1958.

[9] P. H. Leslie and J. C. Gower, "The properties of a stochastic model for the predator-prey type of interaction between two species," *Biometrika*, vol. 47, pp. 219–234, 1960.

[10] R. M. May, *Stability and Complexity in Model Ecosystems*, Princeton University Press, Princeton, NJ, USA, 1973.

[11] D. K. Arrowsmith and C. M. Place, *Dynamical Systems*, Chapman and Hall Mathematics Series, Chapman & Hall, London, UK, 1992.

[12] S. B. Hsu and T. W. Huang, "Global stability for a class of predator-prey systems," *SIAM Journal on Applied Mathematics*, vol. 55, no. 3, pp. 763–783, 1995.

[13] E. Sáez and E. González-Olivares, "Dynamics of a predator-prey model," *SIAM Journal on Applied Mathematics*, vol. 59, no. 5, pp. 1867–1878, 1999.

[14] S.-B. Hsu and T.-W. Hwang, "Hopf bifurcation analysis for a predator-prey system of Holling and Leslie type," *Taiwanese Journal of Mathematics*, vol. 3, no. 1, pp. 35–53, 1999.

[15] P. A. Braza, "The bifurcation structure of the Holling-Tanner model for predator-prey interactions using two-timing," *SIAM Journal on Applied Mathematics*, vol. 63, no. 3, pp. 889–904, 2003.

[16] A. Korobeinikov, "A Lyapunov function for Leslie-Gower predator-prey models," *Applied Mathematics Letters*, vol. 14, no. 6, pp. 697–699, 2001.

[17] J. B. Collings, "The effects of the functional response on the bifurcation behavior of a mite predator-prey interaction model," *Journal of Mathematical Biology*, vol. 36, no. 2, pp. 149–168, 1997.

[18] C. S. Holling, "Principles of insect predation," *Annual Review of Entomology*, vol. 6, pp. 163–182, 1961.

[19] W. Sokol and J. A. Howell, "Kinetics of phenol exidation by washed cells," *Biotechnology and Bioengineering*, vol. 23, pp. 2039–2049, 1980.

[20] Y. Li and D. Xiao, "Bifurcations of a predator-prey system of Holling and Leslie types," *Chaos, Solitons & Fractals*, vol. 34, no. 2, pp. 606–620, 2007.

[21] Y. Kuang, *Delay Differential Equations with Applications in Population Dynamics*, vol. 191 of *Mathematics in Science and Engineering*, Academic Press, Boston, Mass, USA, 1993.

[22] S. Ruan, "On nonlinear dynamics of predator-prey models with discrete delay," *Mathematical Modelling of Natural Phenomena*, vol. 4, no. 2, pp. 140–188, 2009.

[23] Z. Lu and X. Liu, "Analysis of a predator-prey model with modified Holling-Tanner functional response and time delay," *Nonlinear Analysis: Real World Applications*, vol. 9, no. 2, pp. 641–650, 2008.

[24] A. F. Nindjin, M. A. Aziz-Alaoui, and M. Cadivel, "Analysis of a predator-prey model with modified Leslie-Gower and Holling-type II schemes with time delay," *Nonlinear Analysis: Real World Applications*, vol. 7, no. 5, pp. 1104–1118, 2006.

[25] S. Yuan and Y. Song, "Bifurcation and stability analysis for a delayed Leslie-Gower predator-prey system," *IMA Journal of Applied Mathematics*, vol. 74, no. 4, pp. 574–603, 2009.

[26] J.-F. Zhang, "Bifurcation analysis of a modified Holling-Tanner predator-prey model with time delay," *Applied Mathematical Modelling*, vol. 36, no. 3, pp. 1219–1231, 2012.

[27] F. Lian and Y. Xu, "Hopf bifurcation analysis of a predator-prey system with Holling type IV functional response and time delay," *Applied Mathematics and Computation*, vol. 215, no. 4, pp. 1484–1495, 2009.

[28] D. Xiao and S. Ruan, "Multiple bifurcations in a delayed predator-prey system with nonmonotonic functional response," *Journal of Differential Equations*, vol. 176, no. 2, pp. 494–510, 2001.

[29] Z. Liu and R. Yuan, "Bifurcations in predator-prey systems with nonmonotonic functional response," *Nonlinear Analysis: Real World Applications*, vol. 6, no. 1, pp. 187–205, 2005.

[30] F. Shengjin, "A new extracting formula and a new distinguishing means on the one variable cubic equation," *Natural Science Journal of Hainan Teachers College*, vol. 2, no. 2, pp. 91–98, 1989.

[31] J. Guckenheimer and P. Holmes, *Nonlinear Oscillations, Dynamical Systems, and Bifurcations of Vector Fields*, vol. 42 of *Applied Mathematical Sciences*, Springer, New York, NY, USA, 1983.

[32] C. V. Pao, "Dynamics of nonlinear parabolic systems with time delays," *Journal of Mathematical Analysis and Applications*, vol. 198, no. 3, pp. 751–779, 1996.

[33] C. V. Pao, "Convergence of solutions of reaction-diffusion systems with time delays," *Nonlinear Analysis: Theory, Methods & Applications*, vol. 48, no. 3, pp. 349–362, 2002.

[34] T. Faria and L. T. Magalhães, "Normal forms for retarded functional-differential equations with parameters and applications to Hopf bifurcation," *Journal of Differential Equations*, vol. 122, no. 2, pp. 181–200, 1995.

[35] S. N. Chow and J. K. Hale, *Methods of Bifurcation Theory*, Springer, New York, NY, USA, 1982.